HHS Public Access

Author manuscript

Curr Biol. Author manuscript; available in PMC 2022 May 24.

Published in final edited form as:

Curr Biol. 2021 May 24; 31(10): R586–R602. doi:10.1016/j.cub.2021.04.005.

The Many Roles of Myosins in Filopodia, Microvilli and Stereocilia

Anne Houdusse[1,*], **Margaret A. Titus**[2,*]

[1]Structural Motility, Institut Curie, Paris Université Sciences et Lettres, Sorbonne Université, CNRS UMR144, 75005 Paris

[2]Department of Genetics, Cell Biology, and Development, University of Minnesota, Minneapolis, MN 55455

Abstract

An important group of plasma membrane protrusions, filopodia, microvilli and stereocilia, are supported by parallel bundles of actin. These specialized projections have critical roles in sensing the external environment, increasing cell surface area and acting as mechanosensors. While actin-associated proteins are essential for their elongation and bundling, myosins have a surprising role in the formation and extension of filopodia and stereocilia and the organization of microvilli. Actin regulators and specific myosins collaborate in the control of the length of these structures. Myosins can transport cargoes along the length of these protrusions and interactions with adapters and cargoes can also serve to anchor adhesion receptors to the actin-rich core, via functionally conserved motor-adaptor complexes in the case of stereocilia and microvilli. This review highlights recent progress in understanding the diverse roles myosins play in filopodia, microvilli and stereocilia.

Introduction

Filopodia, microvilli and stereocilia are a special class of slender membrane protrusions supported by bundles of crosslinked parallel actin filaments; these protrusions are used by cells to sense and interact with their environments (Fig 1). The actin filaments are organized with their fast-growing (plus or barbed) ends oriented towards the tip and the slower growing (minus or pointed) end embedded in the actin cortex. Filopodia are highly dynamic and found in cells all across the eukaryotic tree, including Rhizaria, Discoba, Apusoza, Amoebozoa and Holozoa, and thus can be considered to be the most ancient of this group of actin-based protrusions [1–4]. Unicellular organisms employ filopodia to physically interact with their environment, mediate substrate adhesion during migration and for capture of prey [5, 6]. While microvilli are present throughout Holozoa, they appear first in unicellular relatives of Metazoa, most notably in Choanoflagellates where they make up the namesake

* co-corresponding authors Anne.Houdusse@curie.fr, Phone: +33 1 56 24 63 95, titus004@umn.edu, Phone: 612-625-8498.

collar that plays a role in feeding [7, 8]. Microvilli provide epithelia with increased surface area for absorption and also serve as a protective barrier [9]. Stereocilia are almost exclusively found in vertebrates where they have essential roles in balance and hearing [8]. Microvilli and stereocilia are tightly linked together by cadherin-based linkages and their lengths are remarkably controlled. Microvilli have a uniform length, that varies from cell type to cell type, whereas stereocilia are graded in height [9, 10]. Each of these projections emerges from the dense, actin-rich cortical cytoskeleton through the action of actin polymerization factors and cross-linkers that work in concert to initiate, extend and bundle the core parallel actin filaments together. A good deal of attention has been paid to the role of the actin regulators in building filopodia, microvilli and stereocilia, but it is now appreciated that myosin motors also play critical roles in both the formation and function of these special structures (Fig 2).

Myosins are a diverse family of actin-based motors found in all major eukaryotic lineages; they can drive intracellular transport, promote contractility, organize actin-based structures, generate tension and aid DNA repair, to name a few functions [11–15]. Myosins can be classified as processive motors, strain-sensitive anchors or tethers, or contractile motors [14]. The function of a given myosin is dictated by a combination of the intrinsic kinetic properties of the conserved motor domain (typically referred to as the “head”) and its interaction with partner proteins determined by varied domains present in their C-terminal tails. The tails also dictate whether the myosin is a monomer, dimer or multimer. A related group of myosins – the MyTH4-FERM (MF; Myosin Tail Homology – Band 4.1, Ezrin, Radixin, Moesin) make significant contributions to the formation and function of filopodia, microvilli and stereocilia. These myosins are characterized by the presence of one (MYO10) or two (MYO7, MYO15) MF domains in their C-terminal tail region that bind to distinct partner proteins required for either transport or anchoring membrane protein complexes[16]. The widespread use of MF myosins to build thin actin-based protrusions reflects both the deep evolutionary conservation of this family of myosins as well as the likely ancient origin of these structures themselves [3, 8]. This review summarizes what is currently known about the pivotal role of myosin motors in the building and activity of filopodia, microvilli and stereocilia.

Myosins in Filopodia Formation and Function

Filopodia are highly dynamic structures that can vary in length from 2 to up to hundreds of μm long and be stabilized by adhesion to neighboring cells or the substrate [17–19]. They play important roles in cellular processes such as adhesion to the extracellular matrix (ECM), guidance towards chemoattractants in development, wound healing and viral infection [17, 20, 21]. Key filopodial proteins and adhesion receptors are present at the tip, where they mediate substrate attachment [22]. They emerge from the cell cortex, which is composed of a branched dendritic network of actin filaments mostly nucleated by the Arp2/3 complex. The overall mechanism of filopodia initiation and extension is highly conserved. Initiation requires activation of a small GTPase, such as Cdc42, as well as actin regulators such as Ena/VASP, a protein with both anti-capping and bundling activity, and/or formins, that nucleate the formation and extension of parallel actin filaments[23]. Filaments are then either reorganized from the cortical network or nucleated de novo so they are oriented perpendicular to the membrane[23] (Fig 3A). A cluster of 10 – 15 actin filaments is minimally

required to overcome membrane tension to push the membrane outwards [24]. Filament extension by Ena/VASP or formins is accompanied by rapid actin cross-linking by proteins such as fascin in mammalian cells. While thin protrusions made by cells are generally all designated as filopodia, it should be noted that filopodia are a diverse group of structures that can be initiated by different mechanisms or have distinctive functions.

Filopodia Initiation.

Two phylogenetically distinct MF myosins are required for filopodia initiation and extension – MYO10 in mammalian cells and DdMyo7 in Amoebozoa[6, 25]. These myosins cluster on the membrane to form initiation sites and localize to the tips of growing filopodia. MYO10 consists of a motor domain followed by a semi-rigid lever arm region that amplifies the swing of the motor as it moves along actin. The lever arm consists of 3 light chain (LC) binding IQ motifs, that bind calmodulin or a calmodulin-like LC, and an elongated stable α-helix (SAH). The lever arm is followed by a dimerization domain that dictates formation of an anti-parallel dimer [26–28]. The MYO10 tail contains 3 PH domains that target MYO10 to PIP3-rich regions of the plasma membrane then a C-terminal MF domain that interacts with various partners, including integrins. The tail of amoeboid DdMyo7, in contrast, contains two MF domains separated by an SH3 domain. Interestingly, functional studies with MYO10 and DdMyo7 show that filopodia formation requires a motor, a post-lever arm region and a dimerization region [25, 26, 29, 30]. Furthermore, the MYO10 MF domain can functionally substitute for a DdMyo7 MF domain [25, 29, 30]. The finding that DdMyo7 and MYO10 share the same general operating principles is consistent with the mechanism of filopodial MF action being evolutionarily conserved.

The requirement for a dimerized motor for filopodia initiation is highlighted by the finding that a forced dimer of either the MYO10 or DdMyo7 motor domain can drive filopodia formation [29, 31]. These two forced dimers lack binding sites for partners, highlighting the critical role of motor function during the initiation step. This does not mean that the tail is entirely dispensable. In the case of the DdMyo7 forced dimer, the resulting protrusions are shorter than wild type filopodia [29], highlighting that the MF domains are needed for the recruitment of elongation factors (see below). An engineered dimeric motor based on MYO6 (MYO6+) that moves towards the plus-end of actin filaments instead of the minus-end can also generate filopodia-like protrusions [32]. Unlike the MYO10 or DdMyo7 forced dimers, MYO6+ requires binding to endosomal membranes mediated by its partner GIPC to make filopodial-like protrusions, suggesting a different mode of operation [29, 32].

Filopodia emerge from MYO10 foci close to nascent focal adhesions rich in actin, integrin and vinculin at the edge of the cell [33, 34]. VASP is also present at these sites where it could work in concert with MYO10 to reorganize Arp2/3 branched actin filaments to initiate filopodia. MYO10 and DdMyo7 are largely cytosolic and exist in an autoinhibited conformation mediated by interactions between the motor and tail region, similar to other myosins [35, 36]. Recruitment to the membrane or cortex relieves autoinhibition, disrupting the head-tail interaction and inducing dimer formation [29, 36]. The exact mechanism by which the head interacts with the tail and how recruitment of the motor occurs by switching the monomer from a compact, closed state to an elongated dimer is not yet understood, although

a role for PIP3 binding has been identified for MYO10 and that of the actin network at the cortex for DdMyo7 [35, 37]. Activation in local clusters favors dimerization of the motor at initiation sites where they can pull on nearby actin filaments, which would favour bundling of actin filaments. This would orient them correctly with their plus-ends abutting the membrane in a position favorable for growth into a filopodium (Fig 3A). The motors can bind to and walk up adjacent parallel actin filaments, zippering them together as they move up towards the plus-ends. The actin filaments are then coalesced into a bundle of sufficient size to push against the membrane, in collaboration with VASP (and/or formin) [38].

Filopodia Elongation and Adhesion.

The initial nucleation/initiation of a filopodium is followed by elongation that depends on MYO10, which switches roles from an organizer of actin filaments at the membrane to a transporter (Fig 3B). MYO10 undergoes intrafilopodial motility and appears to transport VASP towards the filopodia tip [38, 39], where VASP serves to inhibit actin filament capping and promote ongoing polymerization of the growing filaments. The kinetic and structural features of MYO10 are optimized for its function as a transporter on bundles [27, 40]. Dimerized MYO10 is a processive motor that moves most efficiently along bundles of actin filaments at ~ 660 nm/sec with an average run length of 2 μm [27]. These velocities closely match those of MYO10 moving along filopodia in cells, 580 – 840 nm/sec [41]. MYO10 is an anti-parallel dimer [26, 27] that can take variable, large steps (up to 58 nm) preferentially along actin bundles because of both the positioning of the converter domain and extended, flexible lever arm as well as its atypical dimerization. This gives the motor a more flattened orientation relative to the actin filament, enabling the myosin to step across actin filaments in a bundle and take larger steps as it translocates up the filopodium [27]. It should be noted that this structural adaptation is also advantageous for capturing irregularly organized actin filaments at the cortex during filopodia initiation. The overall organization and regulation of MYO10 as compared to other processive motors such as Myo5 reveals how structural adaptations can tune these two motors for best trafficking on distinct cellular tracks [27, 42].

Cells exploit filopodia dynamics to explore the environment; filopodia extend out ahead of the lamellipodium and provide initial contacts with the substrate/ECM via the tip (Fig 3B). Force transmitted along the length of the filopodium by MYH9 (MYO2A) localized at the base stabilizes filopodial contact with the ECM [43]. MYO10 is not only required for filopodia extension but also mediates cadherin- and integrin-based adhesion, binding to receptor cytoplasmic tails via the C-terminal FERM domain and co-localizing with them at filopodia tips[44, 45]. There is currently no direct evidence that MYO10 transports integrins along the length of the filopodial shaft. Rather, it seems that once MYO10 arrives at the tip, it switches from being a transporter to an anchor that traps a small, but critical population of integrin at the tip. Surprisingly, recent work has revealed that the MYO10 FERM domain also binds to the cytoplasmic tail of α-integrin and that binding to both α- and β-integrin tails is important for localized activation of integrins at the filopodia tip [46]. MYO10 binding itself does not activate the integrin as binding to both tails is likely to keep the receptor in a low affinity conformation. Instead, it appears that the myosin anchors the integrin at the tip, positioning it for activation by talin FERM domain binding (Fig 3B), possibly following the influx of Ca^{2+} by L-type channels and subsequent cleavage by calpain [18, 22, 47].

Displacement of MYO10 from the integrin tails by talin would free MYO10 for binding to another integrin or to promote continued filopodia elongation. This displacement would result in adhesion sites forming in the shaft of these specially stabilized filopodia. The mechanism by which the MYO10-filopodia tip complex controls actin polymerization and adhesion in a tension-dependent manner and the composition of the tip itself remains to be characterized.

The essential role of MYO10 in filopodia formation suggested that deletion of this motor would be lethal for a multicellular organism. A large fraction of homozygous *MYO10*$^{tm1d/tm1d}$ or *MYO10*$^{m1J/m1J}$ null mutant embryos die due to exencephaly but a significant number still survive [48, 49]. The brains of surviving *MYO10*$^{-/-}$ embryos do not exhibit any gross abnormalities, but it remains to be seen if these animals have defects in cognitive function [48, 49]. The phenotypes of the surviving *MYO10*$^{-/-}$ mice are consistent with a loss of filopodia, including failed migration of melanocytes resulting in the appearance of a characteristic white belly spot, syndactyly (webbed digits) and abnormalities in the retinal vasculature due to persistent hyaloid vasculature [48, 49]. The surprising survival of the *MYO10*$^{-/-}$ mice and ~50% decrease in filopodia that occurs during retinal angiogenesis indicates that cells and tissues have strategies to bypass the loss of MYO10 and use alternative pathways to make these structures.

MYO10 and Cancers.

Strong upregulation of MYO10 expression is associated with metastatic breast, skin and lung cancers [50–53]. Reduction of MYO10 expression in various metastatic cell lines significantly reduces filopodia production and diminishes invasion in 3D assays. Consistent with the important role of MYO10-induced filopodia in metastasis, induction of malignant melanoma in *MYO10*$^{-/-}$ mice results in smaller tumor size, reduced spread of cancer to the lungs and increased survival compared to control wild type mice [54]. Cancer cells can migrate through the ECM either solo or as part of a cell collective composed of a small population of leader cells at the front and followers that make up the main mass of the collective. Epigenetic changes modify the *Myo10* genomic locus only in leader cells resulting in increased MYO10 protein levels and robust production of filopodia [53]. These cells also secrete high levels of fibronectin (FN1) compared to the followers and as the cells move through the ECM they pull and align the FN1 fibers. This action results in the formation of linear tracts that facilitate more efficient migration of the collective. Filopodia are stabilized by their interaction with FN1 as the front of the leader cells advances and adheres strongly to the ECM. Interestingly, increasing filopodia number in leader cells by overexpression of MYO10 might be predicted to impair migration of the collective by generating more adhesion. However, increased numbers of filopodia enhance migration of the cell collective, which is likely due to increased alignment of the FN1 matrix.

Tunneling Nanotubes and Cytonemes.

Long filopodia-like extensions play critical roles in intercellular communication by serving as conduits for transfer of signals from one cell to another. Tunneling nanotubes (TNTs) and cytonemes are slender (70 – 200 nm diameter) protrusions suspended between cells (i.e. they are not in contact with the substrate) that can reach lengths of 100 μm (TNTs) to 300 μm

(cytonemes)[55, 56]. These hollow tubes contain actin filaments and membrane vesicles, organelles and even pathogens are seen to be actively transported within them. Cytonemes are critical for the long-distance delivery of morphogens such as sonic hedgehog (SHH) to differentiating tissues[56]. TNTs are observed both in cultured cells and tissues where they are typically open-ended at the contact site for each cell. TNTs are implicated in cancer chemoresistance and used for the spread of pathogens and viruses [55]. For example, the HIV-1 accessory protein Nef stimulates MYO10-dependent TNT formation, promoting the cell-to cell spread of the virus[57]. The mechanism of TNT formation is poorly understood although it is thought that they may arise from dorsal filopodia that require MYO10 for their formation. Overexpression of this myosin has been observed to increase both the number of these protrusions and vesicle transfer between cell partners, but whether MYO10 plays a transport role is currently unclear[58]. In contrast, recent work strongly implicates MYO10 as the motor transporting morphogen-containing vesicles along the length of cytonemes to their target cell using cultured mouse cells[59]. The MF domain of MYO10 is essential for its activity, indicating that it is bound to an adapter protein present on SHH-containing vesicles. SHH signaling is critical for neuronal development and it was found that its activity is notably diminished in the neural tube of E9.5 brains of Myo10$^{-/-}$ mice. Interestingly, SHH signalling is not completely lost in these mice, indicating that a redundant or alternative pathway can promote some activation of SHH targets in the absence of cytonemes [59]. The role of MYO10 or related myosins in building both TNTs and cytonemes remains unclear at present.

Future Directions for Filopodia and Myosins.

There remain many open questions about how MYO10 contributes to filopodia formation and activity. Its mechanism of action during filopodia initiation is still undefined. In addition to acting as an actin organizer or a transporter, it might also serve to anchor membrane receptors such as integrins at the filopodia tip. The exact roles MYO10 plays and which factors control the mode of motor functionality is an interesting area for future study. Finally, MYO10 plays an outsized role in filopodia formation in vertebrates making it surprising to find that it is lost in insects and nematodes. These lineages have Myo7 and Myo15 and insects also have Myo22 with two MF domains in the tail[3]. Perhaps one of these myosins could play a role in filopodia formation similar to DdMyo7, as suggested by recent work showing fly Myo7a can bundle actin filaments when dimerized[60]. One of these myosins could also play a role in cytoneme formation. Alternatively, organisms could employ a purely actin-based mechanism for filopodia formation. Thus, the designation ‘filopodia’ likely defines a diverse group of thin cellular protrusions that may or may not require a myosin for formation.

Myosins and Microvilli

The apical surface of epithelial cells that line the lumen of absorptive gut or kidney tubules is covered with a tightly packed carpet of microvilli that make up a brush border (Fig 1 E–H). These projections are supported by a cross-linked core of 20 to 30 tightly bundled actin filaments with their plus-ends at the tip and minus-ends at the end of long rootlets embedded

in a dense terminal web. They are strikingly uniform in length and held together at their tips by cadherin-based linkages.

Microvilli myosins involved in membrane tension.

MYO1A was the first mammalian unconventional myosin discovered. It is a Ca^{2+}-regulated motor with a tail domain that directs binding to acidic lipids such as PIP2 [61], essential for cross-linking the actin core of microvilli to the overlying plasma membrane [62] (Fig 4). Elegant studies established that MYO1A powers the flow of membranes from the base to the plus-end tips of microvilli and promotes the release of vesicles from the microvilli tips into the intestinal lumen [63–65]. These vesicles are enriched with alkaline phosphatase (that likely serve an anti-bacterial function by degrading bacterial lipopolysaccharide) and with key microvilli enzymes such as sucrase isomaltase. Whether this slow (moves at 30 – 60 nm/sec), non-processive monomeric motor is assisted by a partner protein to carry out its functions remains unclear as its high abundance possibly suffice to maintain membrane tension. Surprisingly, in spite of the morphological abnormalities seen for the microvilli and disorganization of the whole brush border seen in MYO1A null mutant mice, they do not exhibit any overt intestinal dysfunction [65]. However, this is likely due to compensation by increased levels of other myosins such as MYO1C in the microvilli core [65]. Loss of MYO1A results in colorectal cancer and it thus also has a role as a tumor suppressor as it is critical for maintenance of polarity of intestinal epithelial cells [66].

Interestingly, a loss of MYO6 localization from intermicrovillar region has been reported in the MYO1A null mutant [65]. MYO6 is tension-sensitive dimeric motor that uniquely moves towards the pointed ends of actin filaments. It serves to traffic receptors and channels to the base of microvilli where they undergo internalization via clathrin-mediated endocytosis. MYO6 thus controls the steady-state levels of proteins such as CFTR and NHE3 in the brush border and loss of this motor correlates with increased levels of the CFTR channel on microvilli membrane [67]. MYO6 also has an important role in maintaining the integrity of the brush border. Mice lacking MYO6 (*sv/sv*) have an irregular brush border where the membrane is no longer pulled down to the very base of the microvilli projections and fusion of microvilli is observed [68]. Interestingly, *Myo1A*$^{-/-}$; *sv/sv* double mutants do not exhibit any membrane tethering defects and the overall morphology and hexagonal packing of microvilli appears normal [69]. The restored morphology is associated with the appearance of MYO1C, D, E and Myo5A in the BB where they most likely compensate for the lack of the other myosins. However, it should be noted that the endocytic defects seen in the *sv/sv* mutant remain. Thus, the action of MYO6, exerting a downward force on the microvilli membrane opposes that of MYO1A and generates membrane flow towards the tip, providing a precise balance of forces to maintain the integrity of the microvilli membrane.

MYO7B-Dependent inter microvillar links.

Microvilli are linked together at their tips by a heterophilic complex of CDHR2 and CDHR5 cadherins [70] (Fig 4). During development of the epithelium, small clusters of microvilli linked together at their tips are seen. As the number of microvilli protruding from the apical surface increase, they are all linked together at their tips, forming a network across the top of the cell [70]. The result is that connections organize the microvilli into a tight, mechanically

integrated network. The cytoplasmic tails of cadherins at the tips of microvilli are anchored to the actin core by the IMAC (inter microvillar adhesion complex). This complex is composed of MYO7B, an MF myosin, the PDZ domain adaptor protein harmonin-1 (USH1C) and the adaptor protein ANKS4B, a complex of proteins strikingly similar to the MYO7A-based Usher I complex found in stereocilia (see below). Microvilli of epithelial cells depleted for MYO7B lack tip localization of IMAC components, notably CDHR2. The inter-microvilli links are then visible along their length instead of just at their tips [71]. Similarly, loss of one of the two MYO7B LCs, CALML4, results in a loss of IMAC tip targeting establishing the critical role of this subunit in motor functionality [72].

The IMAC complex is anchored to the microvilli actin core via the motor domain of MYO7B, providing a mechanism for adjusting tension across the links [70]. Loss of any one IMAC component causes loss of targeting of the other components to the tips and thus loss of the microvilli tip linkages [70, 73]. A network of interactions connects the different members of the IMAC together with the PDZ adaptor protein USH1C playing a key role. High resolution structures of the ANKS4B central intrinsically disordered region (CEN) binding to MYO7B MF1 and the USH1C PDZ3 to MYO7B MF2 suggest how the adaptor-motor IMAC complex is assembled[70, 74–76]. In fact, several distinct complexes are possible given the number of interaction sites between the different players [76]. Consistent with the multivalent interactions within the IMAC, a 1:1:1 mixture of USH1C, ANKS4B and the MYO7B MF tail domains can form a condensate both *in vitro* and when ectopically expressed in HeLa cells via liquid/liquid phase separation [77]. There is a cap of electron dense material at the tips of microvilli that could correspond to an IMAC condensate, providing a high local concentration of connections between cadherin and the actin cytoskeleton. Such a robust anchorage of the inter-microvilli cadherin links is critical for the brush border to withstand the mechanical stresses regularly experienced by the intestinal epithelium.

MYO7B is implicated in mediating IMAC functions in two different ways: transport of the complex to the tip and anchoring to actin to link microvilli tips to each other [71, 73]. Movement of MYO7B towards the tip of a microvillus has been observed and loss of motor activity eliminates the formation of connections between microvilli tips, resulting in the disorganization of microvilli [71]. An *in vivo* ‘pull-down’ strategy showed that ANKS4B, USH1C and the cytoplasmic domains of either CDHR2 or CDHR5 can bind to the MYO7B tail independently, suggesting that MYO7B could transport these components individually to the tip[78]. The exact nature of the cargo that MYO7B transports to the microvilli tip (a subset of components, or all of them) is not known. MYO7B has relatively low ATPase activity but a high duty ratio as is typical for motors that can act as tethers or anchors [79]. The clear localization of MYO7B to the microvilli tip also suggests that it must have dual roles as both a transporter and an anchor. A key question then is what triggers the switch from a transporter to an anchor and whether the MYO7B motor switches from operating as a dimer to functioning as a monomer? Such a switch might occur when the motor experiences a higher load which likely requires the reorganization of the transported complex when it reaches the tip[76]. This could occur as higher local concentration of IMAC components would favour integration into a dense network by liquid/liquid phase separation. How MYO7B motor activity affects the formation or stability of the condensate is currently

undefined. Further studies are required to identify the factors that determine the precise position and geometry of the microvilli tip links during brush border maturation phase together with the formation of the associated IMAC electron dense regions.

The length of microvilli on a single cell is strikingly uniform, exhibiting only 5% > SD variation of the mean length (~ 1.1 μm) in the mouse small intestine, for example [65]. How is this length so precisely maintained? There appears to be complex interplay between myosin-generated force, actin polymerization and intermicrovillar links that determine the consistent microvilli height across the brush border. Non-muscle myosin IIC (MYH14 - referred to here as MYO2C) is specifically enriched in brush border fractions where it is localized to the actin rootlets of microvilli, as well as at adherens junctions [80, 81]. Surprisingly, inhibition of MYO2C causes elongation of microvilli, disorganization of the BB and a substantial reduction of the retrograde flow in the microvilli core in W4 cells, a useful model for early epithelial cell morphogenesis. Ectopic overexpression of MYO2C, on the other hand, results in dramatic shortening of microvilli and mutations in the motor domain abrogate this phenotype [80]. These findings strongly implicate MYO2C contractility, pulling on microvilli actin rootlets in the terminal web region. The effect of MYO2C on the retrograde flow of the actin bundle indicates that this motor counteracts addition of actin monomers to the tip by promoting an optimal level of depolymerization at the rootlets (Fig 4). MYO7B may also play a role in controlling microvilli length. The *Cdhr2*$^{-/-}$ mutation results in a significant reduction in microvilli height, about 50% shorter. The loss of the CDHR2-based links distorts the shape of the microvilli, instead of its usual circular outline the mutant microvilli are more oblong and the actin core appears irregular. The close packing of microvilli is also significantly disrupted[82]. Thus, transport of CDHR2 to the tip of microvilli may be crucial for dictating the coordinated length of adjacent protrusions. Co-expression of a chimeric MYO10-motor:MYO7B tail and CDHR2 in HeLa cells robustly produces filopodia. Interestingly, filopodia tips enriched in CDHR2 and the chimeric motor appear to be gathered together with several of them being matched in height. Occasionally, one filopodia tip can be observed to slide along the side of another until it reaches the tip and stops growing [78]. While this heterologous system is obviously lacking the normal actin regulators that build microvilli, these intriguing findings implicate the tension generated from the two tips being linked together as another potential player in precisely controlling and matching the height of adjacent microvilli.

Myosins of the Stereocilia

The sensory cells of the auditory and vestibular epithelia in vertebrates are characterized by the presence of specialized apical projections known as hair bundles. Each contains 50–100 actin-filled stereocilia, arranged in ranks of successively increasing height, giving the bundle a staircase-like appearance (Fig 1I–L). The stereocilia are modified microvilli that can be up to 120 μm in length [83]. The sensory hair cells of the inner ear have distinct functions – vestibular hair cells for balance, cochlear inner and outer hair cells (IHC, OHC) for hearing by frequency detection – and organization in different parts of the inner ear (vestibular versus cochlear) [84]. During hair cell development, formation of the hair bundle involves establishment of planar polarity, building of stereocilia that are organized into their typical architecture, precise specification of stereocilia lengths and formation of stereotypical links

that join stereocilia together [85, 86]. The acquisition of mechanotransduction and how that influences development of the hair bundle is also important for stereocilia maturation [87, 88]. Given the complexity of the system, this review will confine itself to an overview of what is known about the function of myosins in IHCs [10, 85, 88, 89].

The hair bundle is a mechanotransducer comprised of stereocilia that converts sound waves or orientation information into electrical signals [90]. Stereocilia are membrane protrusions supported by a parallel bundle of actin filaments oriented with their minus-ends in the rootlets that anchor them in the apical region of the hair cell. They are wider than microvilli, tapered at the bottom, ordered in rows of graded height. The overall height of the bundle varies along the length of the sensory epithelium. Connections between stereocilia link them into an integrated bundle that acts as a single transduction unit. In the mouse cochlea, there are three rows of stereocilia (row 1 is the tallest) and the tops of shorter stereocilia in rows 2 and 3 are linked to the side of the adjacent taller stereocilia via a cadherin-based structure known as the tip link (Fig 5). The cadherin PCDH15 makes up the lower half of the tip link, which is embedded in the top of the shorter stereocilia and is associated with the mechanotransduction channel (MET). The cadherin CDH23 composes the upper half of the tip link; its membrane-spanning domain is embedded in the side of the taller, adjacent stereocilia. Sound waves causes a deflection of the bundle in the direction of taller stereocilia that pivots at its base. The resulting strain transmitted via the tip-link opens the MET channel, allowing ions to flow into the stereocilia [90].

Genetic approaches have made substantial contributions to identifying roles for myosins in the hair cell, most notably uncovering the identity of genes mutated in Usher syndrome, the leading cause of combined deafness and blindness in the human population, and characterization of mouse deafness genes [85]. A combination of elegant biophysical, cell biological and single cell proteomic studies has identified a diverse group of myosins required for stereocilia linkages, growth, length control and mechanotransduction (Fig 5).

Myosins in adaptation and channel gating.

Opening of the MET channel causes depolarization of the cell followed by slow Ca^{2+} and actin-dependent adaptation. This resets tip link tension and leads to MET channel closing, allowing it to operate at maximum sensitivity. A series of elegant biophysical and chemical genetic studies revealed a role for MYO1C in slow adaptation [91]. MYO1C is a monomeric motor regulated by Ca^{2+} with a PIP2 binding domain in its tail that is localized to the upper tip link density. A related Myo1 family member, Myo1H, is present in the hair bundle at similar levels as MYO1C and also appears to be localized to stereocilia tips [92]. A small ensemble of MYO1C is thought to anchor the tip link to the stereocilia actin core by binding to the tail of CDH23 [91]. When tension is applied to the tip link, this non-processive motor slips down the actin core, reducing tension across the link and allowing the MET channel to close (i.e. adaptation). It is unknown, however, how Myo1H contribute to this process, how MYO1C motors cluster when bound to PIP2, and if other membrane-associated proteins are required for their organization or to connect them to the upper tip link.

MYO7A is localized to the upper tip-link density (UTLD) and early work implicated this motor in MET channel transduction [93, 94]. *Myo7a*$^{6J/6J}$ hair bundles exhibit abnormal

mechano-electrical transduction, but as they are mildly disorganized, it has been difficult to solely ascribe the defects to impaired MET gating [94]. Gene edited mice that lack the canonical MYO7A isoform (−ΔC) have significantly reduced levels of MYO7A protein only in IHCs, with a loss of 60–70% from the UTLD, yet maintain hair bundle integrity. The *Myo7a*-ΔC hair bundles exhibit a significant delay in the initial onset of current, consistent with the loss of a tension on the tip link [95]. The progressive deafness that results from the loss of the long MYO7A isoform might be linked to a lower expression of MYO7A motors in these *Myo7A*-ΔC hair bundles. Alternatively, the 11 amino acid difference in the Nter myosin sequence could result in drastically different motor properties under load, as has been seen for other myosins such as Myo1B and Myo14 [96, 97]. These findings implicate MYO7A in tensioning the MET channel through anchoring the upper tip link to the actin core of the stereocilia and potentially providing a mechanically sensitive response to applied tension following hair bundle deflection. Further studies are needed to clarify how MYO7A anchoring properties are modulated either by Ca^{2+}-signaling or tension to maintain and adjust tip link tension.

Myosins Anchoring stereocilia links and the plasma membrane.

Top connectors, shaft connectors, lateral links and ankle links hold the hair bundle together [85]. Early studies revealed that these are calcium-sensitive, implicating cadherin family members as key components [98]. The MF myosin MYO7A is localized all along the stereocilia length with concentrations where cadherin-based connectors link adjacent structures, at ankle links near the bottom of the stereocilia and at the upper tip link density [93, 99, 100] (Fig 5). Mutations in the *Myo7a* gene in Usher syndrome type IB patients and the *sh1 Myo7A* mouse mutant establish this myosin as a central player in the formation and maintenance of a number of interstereociliary links [101, 102]. The hair bundles from cochlear hair cells are notably disorganized and splayed apart in *sh1* mice, similar to what is seen for the zebrafish *Myo7a mariner* mutant [103, 104].

Characterization of Usher syndrome Type I mutations led to the identification of a protein complex composed of USH1C (Harmonin), USH1G (SANS) and MYO7A that anchors the cadherin links of the stereocilia to the underlying actin core of the stereocilia, similar to the microvilli IMAC [85]. The multi-PDZ protein Harmonin is also a central player in this complex – it can interact with the cytoplasmic tail of CDH23 at the upper tip link density (UTLD), SANS and MYO7A MF1 via canonical and non-canonical PDZ domain interactions and its C-terminal PDZ3 domain interacts with MYO7A MF2[76, 105, 106]. Interestingly, the short Cter extension of Harmonin PDZ3 also binds to its own PDZ1, an interaction that promotes an autoinhibited state that could serve to control interactions with MYO7A or SANS [76, 107]. As seen for the IMAC proteins, when ectopically expressed in HeLa cells, the MYO7A tail, SANS and Harmonin-1a form a cytosolic liquid condensate upon liquid/liquid phase separation[77]. Interestingly, this condensate is abrogated by deafness-causing mutations in the MYO7A tail known to disrupt binding to the PDZ3 domain of Harmonin[77], consistent with strong, multivalent interactions between these proteins playing a critical role in the formation of the dense condensate.

CDH23 is linked to MYO7A through Harmonin at the UTLD. Disruption of the CDH23 binding site or a complete loss of all Harmonin isoforms disrupts the organization of cochlear hair cell bundles and alters the speed and extent of adaptation [108, 109], establishing the important role of Harmonin in the stable formation of inter-stereociliary links and mechanotransduction. There are a number of different Harmonin isoforms expressed in the cochlear and vestibular sensory epithelia and these have the potential to interact with a diverse set of binding partners [110]. While the interactions with SANS and the N-terminal MYO7A MF1 domain are conserved whatever the isoform, the potential for actin bundling or for binding to the MYO7A MF2 domain differs among isoforms. Thus, the varied interactions between these proteins might lead to different mechanical properties for this network depending on the isoforms present[75, 76, 99, 106, 111]. A key question is what regulates the clustering of MYO7A motors via the formation of complexes in a Harmonin-isoform dependent manner. Changes in the expression of individual Harmonin isoforms or their levels are likely to play a role in dictating the type of MYO7A complex formed, but the presence of other binding partners is possibly also an important determinant (see below). Comprehensive cataloging of isoforms in hair bundles throughout development by single cell proteomics and transcriptomics will undoubtedly provide answers to some of these questions in the near future [92, 112, 113].

An outstanding question is whether MYO7A serves as a transporter, bringing USH complex members to various sites of action. MYO7A is a monomer which is regulated by head-tail autoinhibition, the Cter FERM domain inhibits activity by binding to the motor domain [114]. MYO7A alone does not translocate along filopodia in HeLa cells but when co-expressed with a binding partner, MyRIP, both move to the tips of filopodia [115]. This finding suggests that cargo binding both relieves autoinhibition and dimerizes (or oligomerizes) the motor allowing it to translocate along parallel actin filaments. One can envision that binding of Harmonin/SANS to the tail could also promote MYO7A dimerization to serve a similar function.

MYO7A has been found to bind to other transmembrane adhesion linkers. Usher syndrome Type II (USH2) is characterized by moderate hearing loss and retinitis pigmentosa. It results from mutations in two distinct transmembrane adhesion linkers, ADGVR1 (Vlgr1/GRP98; USH2C) and Usherin (USH2A), that are components of the ankle link [116]. Cochlear hair cells of mice lacking ADGVR1 exhibit significant disorganization [116]. MYO7A interacts with the cytoplasmic domains of Usherin and ADGVR1, via its MF2 domain. Both are lost from ankle links in *Myo7a* mutants, illustrating the central role that this motor has in either establishing and/or maintaining these connections [116, 117]. Similar to what is seen with the USH1 complex, the cytoplasmic tails of the USH2 proteins interact with PDZ domain cytosolic adaptors, WHRN (whirlin, USH2D) and PDZD7 which also bind to the MYO7A tail[116–118]. Mutations in WHRN and PDZD7 are associated with deafness[119, 120]. The transmembrane protein Vezatin is also present in ankle links where it interacts both with the cytoplasmic tail of Usherin and the MYO7A MF2 domain[116, 121]. Thus, MYO7A is a core component of multiple, distinct complexes critical for the formation and maintenance of ankle links at the base of stereocilia, which are integral for the cohesion of the hair bundle. The diversity of interactions suggests a sophisticated mechanism for the timely formation and targeting of each complex throughout the development and lifespan of sensory hair cells.

Separation of individual stereocilia is maintained by anchoring of the apical membrane to the actin-dense cuticular plate that anchors the actin rootlets. MYO6 is found both in the cuticular plate and at the tapered base of the stereocilia. In the *sv/sv Myo6* mutant, bulging of the membrane between stereocilia and club-like fused stereocilia are observed[122–124]. Thus, MYO6 plays a pivotal role in anchoring the stereocilia membrane to the cuticular plate, similar to its role in tethering the membrane to the base of microvilli[68]. MYO6's role in anchoring the membrane may be due to its role in endocytosis at the base of stereocilia (and microvilli) and/or in stabilizing the basal links between adjacent stereocilia as *sv*/*sv* mutants exhibit a redistribution of basal linker proteins from the base to the shaft of the stereocilia [125–127].

Myosins control stereocilia length.

The length of individual stereocilia is precisely regulated both within the hair bundle and throughout the sensory epithelium (e.g. along the length of the cochlea). Myosin activity contributes to stereocilia elongation via the delivery of actin regulators to their growing tips or by controlling the activity of actin regulators (Fig 5). In addition, several different myosins interact with the cytoplasmic domain of tip links and loss of these myosins or inhibition of MET channel activity impacts stereocilia elongation. Thus, the control of stereocilia length requires a delicate partnership between actin dynamics, myosin activity and mechanotransduction, revealing that function and development are intertwined.

MYO3A and MYO3B regulate stereocilia extension where they associate with actin bundlers ESPN-1 and ESPNL that accumulate at stereocilia tips [128]. They are unusual hybrid myosins with an N-terminal Ser/Thr kinase domain, a central (actin-binding) motor domain and a short C-terminal tail region, distinguished by the presence (3A) or absence (3B) of an actin-binding domain (THDII). These myosins are regulated by autophosphorylation and phosphorylation of the motor significantly decreases affinity for actin, reducing motor activity [128, 129]. MYO3A and B are monomeric; yet when a kinase dead MYO3A is expressed in HeLa cells, it moves slowly along the length of filopodia to the tip, slowing filopodia dynamics and enhancing filopodia lifetime [130, 131]. Mutations in the actin THDII actin binding domain abolish this activity, revealing that tail binding allows the myosin to move along the actin filament in an 'inchworm' type fashion [131, 132]. Co-expression of MYO3A and ESPN-1 in HeLa cells promotes filopodia elongation [131]. In contrast, MYO3B alone does not localize to filopodia tips in COS7 cells, consistent with the absence of the THDII domain. However, when co-expressed with ESPN-1 the two proteins are found at the tips and increased filopodia extension occurs [133]. Mutation of the actin binding motif in ESPN-1 abolishes the tip localization of MYO3B, revealing that ESPN-1 provides a second actin binding site that allows MYO3B to move along actin filaments. The key role of the motors when binding ESPN-1 is not only the transport but also the activation of this actin regulator at the tip of stereocilia. The shared THDI tail region binds to the ankyrin repeat region of ESPN-1, relieving autoinhibition, enabling bundling of actin filaments [134].

MYO3A, 3B and ESPN-1 localize to the tips of stereocilia in a thimble-like distribution while ESPNL is found only at the tips of rows 2 and 3 (the shorter stereocilia; [133, 135, 136]).

Loss of MYO3A results in late onset deafness in human patients (DFNB30) and in mice[137–139], while MYO3B and ESPN-1 mutants do not exhibit any loss of hearing although the slope of the hair bundle staircase is altered in a subset of vestibular cells in the ESPN-1 nulls[135]. In the case of the ESPN-1 mutant, loss of the activity of this one isoform is likely compensated for by the related ESPNL. MYO3A is not essential for stereocilia formation but its loss results in degeneration after several months [139]. Stereocilia are then misshapen and in fact are longer than controls revealing that MYO3A has a role in setting the final length of these protrusions [135, 137, 139]. In contrast, a subtle decrease in the length of the shorter stereocilia is observed in the *Myo3B*$^{-/-}$ mutant. The *Myo3A*$^{-/-}$ *Myo3B*$^{-/-}$ double mutant mice are profoundly deaf and exhibit global dysregulation in stereocilia organization and length with a loss of the graded height typically seen in hair bundles [137]. Thus, MYO3A and B are not required for stereocilia formation but rather have shared roles in fine-tuning actin dynamics for setting or maintaining the proper stereocilia graded length required for function.

Myosin control over the graded height of stereocilia.

Tremendous progress has been made in understanding how the lengths of the stereocilia in each row are specified and in identifying the key players required for elongation and maintenance of the distinct rows. Loss of the MF myosin MYO15A (Fig 2) in the *shaker-2* (*sh2*) mutant results in strikingly short stereocilia of uniform height of both cochlear and vestibular sensory hair cells, implicating this myosin as a key player in elongation and maintenance of stereocilia length [140, 141]. The *sh2* mutation (C1779Y) likely disrupts nucleotide binding at the P-loop of MYO15A, establishing that its motor activity is essential for function [141]. Dimerized MYO15A moves at 300 nm/sec and kinetic analysis demonstrates that MYO15A has a moderate duty ratio [142, 143]. Ectopically expressed MYO15A moves towards the tips of filopodia in COS7 cells, consistent with a role as a stereocilia transporter [142, 144]. The ability to translocate to filopodia tips suggests that it can either dimerize or has a second actin binding site in its tail, similar to MYO3A. There are two MYO15A isoforms (MYO15A-L and MYO15A-S) that differ by the presence or absence of a ~1208 aa long N-terminal extension predicted to be largely disordered (but possibly involved in binding partners) [145]. The expression of these two MYO15A isoforms is temporally and spatially regulated during development [146]. During the early stages of stereocilia maturation both isoforms are uniformly localized to the tips. However, maturation of the hair bundle towards a graded height stereocilia arrangement is correlated with MYO15A-S being exclusively on the tips of the tallest stereocilia in row 1 and MYO15A-L on the tips of the shorter rows (2 and 3) where the MET channel resides (Fig 5). The differential localization of the two isoforms implicate the N-terminal region in regulating targeting of MYO15A-L to the shorter rows by a mechanism that is not clear.

Careful and systematic analysis of a cohort of mouse mutants with phenotypes similar to those of *sh2* has revealed a critical role for MYO15A in specifying row 1 height and dissected key players in regulating and maintaining row 1 identity. IHCs lacking either EPS8 (a regulator of actin dynamics), WHRN (a PDZ protein), GPSM2 (a GoLoco protein) or GNAI3 ($G\alpha_{i3}$, the α subunit of a heterotrimeric G protein) have an identical phenotype – short, immature hair bundles with excess stereocilia[146–150]. The mutant IHCs are similar in

appearance to the immature hair cells (E18.5) that also have a shallow staircase morphology and excessive stereocilia. These five proteins form a complex that is mainly localized to row 1 during maturation. MYO15A binds to the C-terminal PDZ domain of WHRN via a PBM (PDZ binding motif) that resides at its very C-terminus and its MF2 binds the PTB domain of EPS8. MYO15A appears to have a critical role in transporting EPS8 and WHRN to the tips of stereocilia, as both are lost from the tips of row 1 stereocilia in the *sh2* mutant, but MYO15A localization is not altered in the $wi^{-/-}$ mutant [144, 148]. MYO15A-L and WHRN are co-transported to the tips of filopodia in COS7 cells, and when EPS8 is also present, filopodial extension is enhanced. This is consistent with a MYO15A:WHRN:EPS8 complex promoting the extension of parallel actin bundles [144, 148]. Both WHRN and EPS8 are enriched at the tips of the tallest stereocilia, and the levels of MYO15A-S and WHRN are directly correlated [146, 147]. A GSPM2-GNAI3 complex is required to stabilize the MYO15A-S:EPS8:WHRN complex at the tip of row 1 stereocilia. Loss of either GPSM2 or GNAI3 results in a loss of row 1 identity and height differential across the three rows with MYO15A-L and Esp8 now at the tips of all stereocilia rows [149, 150]. The signaling events that result in selective recruitment and stabilization of GSPM2 and GNAI3 to row 1 and how they, in turn, stabilize the MYO15A-S:EPS8:WHRN complex are not yet known. The selective localization of WHRN and EPS8 to row 1 stereocilia by MYO15A-S is unexpected, given that MYO15A-L and -S both have a Cter PBM. This reveals that the interaction between the MYO15A isoforms and their cargoes is tightly controlled in a context-dependent manner. The N-terminal extension of MYO15A-L interacts with the tail to prevent binding of certain cargoes (such as WHRN or EPS8) and perhaps this autoinhibitory interaction specifically blocks interaction of the PBM with WHRN [146].

Recent work showed that the MF2-PBM binding region of MYO15 can form a dense codensate with WHRN and the N terminal PTB-WBD of EPS8 both in vitro and when all three proteins are ectopically expressed in cells, similar to what is seen for the MYO7A and B tails and their partners Harmonin and SANS/ANKS4B (Fig 2)[77, 151]. The ability of EPS8 to bind actin and the presence of dense material at the tip of stereocilia suggests that a MYO15-mediated condensate could serve to anchor actin filaments to the membrane at the tip. Interestingly, the condensate does promote actin bundling in vitro with droplets seen to be decorating the filaments. Much remains to be learned about the interactions between MYO15, WHRN and EPS8 and their potential role in linking it to the stereocilia tip. As is the case with MYO7A and B, it remains to be seen how myosin motor activity may impact complex assembly and transport as well as condensate formation.

Role of Mechanotransduction.

The development of the cochlear IHC hair bundles in mice involves both widening and lengthening of stereocilia that occurs in alternate phases[152]. The first lengthening phase occurs during embryonic development, this is followed by widening, with row 2 increasing most notably (P0-P4.5). Then, a second phase of stereocilia lengthening occurs, with row 1 dramatically lengthening to 6 μm (P7.5 – 19.5) [87]. The widening phase for row 2 stereocilia correlates with the onset of mechanotransduction. Mutants lacking mechanotransduction due to loss of transmembrane-like channels TMC1 and TMC2 or their targeting partner TMIE exhibit distinct alterations in hair bundle morphology. Notably, the staircase morphology is

less significant and widening of row 2 stereocilia that occurs concomitantly with the onset of mechanotransduction is no longer observed. While some differences are observed between the channel mutants, MYO15A-S, EPS8, WHRN and GNAI3 all are present at stereocilia tips in both row 1 and row 2, with the shift in distribution becoming more pronounced as development proceeds from P7.5 to P21.5. This change appears specific for these row 1 proteins since the tip localization of MYO3A and ESPN-1 is unchanged. Loss of mechanotransduction also impacts the MYO15A-L localization, which then becomes present at the tips of stereocilia in all rows. Interestingly, *sh2* mutants show defects in stereocilia widening in IHCs (and OHCs) resulting in equal diameter stereocilia in all three rows, similar to what is seen in the transduction mutants [153] while the normal changes in stereocilia widening or thinning are maintained in the $Myo15A^{\Delta N/\Delta N}$ mutant specifically lacking the MYO15A-L isoform. Thus, in addition to playing a key role in the graded height of stereocilia, MYO15A-S is critical for controlling the programmed changes in their width. The mechanism by which the protein distribution changes at the tip during the onset of mechanotranduction and how altering the specification of row 1 on actin dynamics promotes increasing stereocilia thickness in row 2 during the onset of mechanotransduction is unclear at present [87, 153]. Together these findings establish that there is an exquisite balance between mechanotransduction and development of the mature hair bundle architecture that relies on MYO15A-S dependent elongation of row 1.

Summary and Perspective

The formation and function of filopodia, microvilli and stereocilia requires a variety of myosin family members with distinct roles that coordinate their action with regulators of actin polymerization. The MF family of myosins play particularly prominent roles in promoting or regulating the growth of these structures (MYO10 - filopodia; MYO15 - stereocilia) and in anchoring adhesion receptors to their actin core (MYO10 - integrin; MYO7, MYO15 - cadherin family members). With their motor activity, these myosins power their translocation along these special actin-based structures, enabling them to deliver actin regulators to their tips, transport channels, membrane or receptors along their length to the tip or the base. Many are localized to specific regions of filopodia, microvilli and stereocilia where anchoring or adhesion receptors reside. There, they can act as tension-sensitive anchors that sense and respond to mechanical changes during extension or bundling of the protrusion. MYO1 and MYO6 also have roles in in driving membrane flow or anchoring the membrane to the actin-rich apical surface of epithelial cells, in addition to anchoring proteins to the actin core. Retrograde flow of the core actin filaments is important for regulating extension or generating tension along the length of filopodia and microvilli, which contributes to stabilize the protrusion and regulate its growth. The diverse motor properties of all of these myosins make each well-tuned to serve their function as either a transporter or an anchor in filopodia, microvilli and stereocilia. The exact role that each motor plays is also defined locally and temporally, depending on the association with specific partners.

Many fundamentally important questions remain about the function of myosins in filopodia, microvilli and stereocilia. There is a delicate balance between protrusion, formation and stabilization; yet the chemical and mechanical signaling that controls the activity of motors

and actin polymerisation factors required for these processes are not fully defined. The timely formation of protrusions relies on the activities of closely related homologs or different isoforms of both the myosin motors and their adaptors, especially in the case of microvilli and stereocilia (e.g. MYO15A-S and -L). The spatiotemporal control of isoform expression and of their activity is poorly understood at present. For example, what determines expression of specific proteins to define the different stereocilia rows and which factors determine onset of elongation and widening phase are some of the most intriguing questions. There are also many gaps in our knowledge about the biochemical properties of the different isoforms and how these impact protrusion function and the composition of various complexes at tips and sites of adhesion. Thus, much remains to be learned about how motors build filopodia, microvilli and stereocilia and contribute to their function. Progress in the coming years will undoubtedly uncover new principles of motor operation and how motors and their tracks work together.

Acknowledgements

AH is supported by an IRP grant from CNRS, ANR-17-CE11–0029-01, ANR-19-CE11–0015-02. The AH team is part of the Labex Cell(n)Scale (ANR-11-LABX-0038), which is part of the IDEX PSL (ANR-10-IDEX-0001–02). MAT is supported by the NIH National Institute of General Medical Sciences (R01GM122917).

Literature Cited

1. Cavalier-Smith T, and Chao EE (2003). Phylogeny and classification of phylum Cercozoa (Protozoa). Protist. 154, 341–358. [PubMed: 14658494]
2. Hanousková P, Táborský P, and Čepička I (2019). Dactylomonas gen. nov., a novel lineage of Heterolobosean flagellates with unique ultrastructure, closely related to the Amoeba Selenaion koniopes Park, De Jonckheere & Simpson, 2012. J Eukaryot Microbiol. 66, 120–139. [PubMed: 29791056]
3. Kollmar M, and Muhlhausen S (2017). Myosin repertoire expansion coincides with eukaryotic diversification in the Mesoproterozoic era. BMC Evol Biol. 17, 211. [PubMed: 28870165]
4. Yabuki A, Ishida K, and Cavalier-Smith T (2013). Rigifila ramosa n. gen., n. sp., a filose apusozoan with a distinctive pellicle, is related to Micronuclearia. Protist. 164, 75–88. [PubMed: 22682062]
5. Parra-Acero H, Harcet M, Sánchez-Pons N, Casacuberta E, Brown NH, Dudin O, and Ruiz-Trillo I (2020). Integrin-mediated dhesion in the unicellular holozoan *Capsaspora owczarzaki*. Curr. Biol. 30, 4270–4275.e4. [PubMed: 32857975]
6. Tuxworth RI, Weber I, Wessels D, Addicks GC, Soll DR, Gerisch G, and Titus MA (2001). A role for myosin VII in dynamic cell adhesion. Curr. Biol. 11, 318–329. [PubMed: 11267868]
7. Dayel MJ, and King N (2014). Prey capture and phagocytosis in the choanoflagellate Salpingoeca rosetta. PLoS One. 9, e95577. [PubMed: 24806026]
8. Sebe-Pedros A, Burkhardt P, Sanchez-Pons N, Fairclough SR, Lang BF, King N, and Ruiz-Trillo I (2013). Insights into the origin of metazoan filopodia and microvilli. Mol. Biol. Evol. 30, 2013–2023. [PubMed: 23770652]
9. Crawley SW, Mooseker MS, and Tyska MJ (2014). Shaping the intestinal brush border. J. Cell Biol. 207, 441–451. [PubMed: 25422372]
10. Barr-Gillespie PG (2015). Assembly of hair bundles, an amazing problem for cell biology. Mol. Biol. Cell. 26, 2727–2732. [PubMed: 26229154]
11. Coluccio LM (2020). Myosins, (Cham, Switzerland: Springer) 455 pp.
12. Cook AW, and Toseland CP (2021). The roles of nuclear myosin in the DNA damage response. J. Biochem. in press.

13. Masters TA, Kendrick-Jones J, and Buss F (2017). Myosins: domain organisation, motor properties, physiological roles and cellular functions. Handb Exp Pharmacol. 235, 77–122. [PubMed: 27757761]

14. Robert-Paganin J, Pylypenko O, Kikuti C, Sweeney HL, and Houdusse A (2020). Force generation by myosin motors: a structural perspective. Chem Rev. 120, 5–35. [PubMed: 31689091]

15. Trivedi DV, Nag S, Spudich A, Ruppel KM, and Spudich JA (2020). The myosin family of mechanoenzymes: from mechanisms to therapeutic approaches. Annu. Rev. Biochem. 89, 667–693. [PubMed: 32169021]

16. Weck ML, Grega-Larson NE, and Tyska MJ (2017). MyTH4-FERM myosins in the assembly and maintenance of actin-based protrusions. Curr. Opin. Cell Biol. 44, 68–78. [PubMed: 27836411]

17. Gallop JL (2020). Filopodia and their links with membrane traffic and cell adhesion. Semin. Cell. Dev. Biol. 102, 81–89. [PubMed: 31843255]

18. Jacquemet G, Baghirov H, Georgiadou M, Sihto H, Peuhu E, Cettour-Janet P, He T, Perälä M, Kronqvist P, Joensuu H et al. (2016). L-type calcium channels regulate filopodia stability and cancer cell invasion downstream of integrin signalling. Nat Commun. 7, 13297. [PubMed: 27910855]

19. McClay DR (1999). The role of thin filopodia in motility and morphogenesis. Exp Cell Res. 253, 296–301. [PubMed: 10585250]

20. Aliyu IA, Kumurya AS, Bala JA, Yahaya H, and Saidu H (2020). Proteomes, kinases and signalling pathways in virus-induced filopodia, as potential antiviral therapeutics targets. Rev Med Virol. eRMV2202. [PubMed: 33314425]

21. Heckman CA, and Plummer HK (2013). Filopodia as sensors. Cell. Signal. 25, 2298–2311. [PubMed: 23876793]

22. Jacquemet G, Stubb A, Saup R, Miihkinen M, Kremneva E, Hamidi H, and Ivaska J (2019). Filopodome Mapping Identifies p130Cas as a Mechanosensitive Regulator of Filopodia Stability. Curr. Biol. 29, 202–216.e7. [PubMed: 30639111]

23. Yang C, and Svitkina T (2011). Filopodia initiation: focus on the Arp2/3 complex and formins. Cell Adh Migr. 5, 402–408. [PubMed: 21975549]

24. Mogilner A, and Rubinstein B (2005). The physics of filopodial protrusion. Biophys. J. 89, 782–795. [PubMed: 15879474]

25. Bohil AB, Robertson BW, and Cheney RE (2006). Myosin-X is a molecular motor that functions in filopodia formation. PNAS. 103, 12411–12416. [PubMed: 16894163]

26. Lu Q, Ye F, Wei Z, Wen Z, and Zhang M (2012). Antiparallel coiled-coil-mediated dimerization of myosin X. PNAS. 109, 17388–17393. [PubMed: 23012428]

27. Ropars V, Yang Z, Isabet T, Blanc F, Zhou K, Lin T, Liu X, Hissier P, Samazan F, Amigues B et al. (2016). The myosin X motor is optimized for movement on actin bundles. Nature Comm. 7, 12456.

28. Vavra KC, Xia Y, and Rock RS (2016). Competition between coiled-coil structures and the impact on Myosin-10 bundle selection. Biophys. J. 110, 2517–2527. [PubMed: 27276269]

29. Arthur AL, Songster LD, Sirkia H, Bhattacharya A, Kikuti C, Borrega FP, Houdusse A, and Titus MA (2019). Optimized filopodia formation requires myosin tail domain cooperation. PNAS. 116, 22196–22204. [PubMed: 31611382]

30. Petersen KJ, Goodson HV, Arthur AL, Luxton GW, Houdusse A, and Titus MA (2016). MyTH4-FERM myosins have an ancient and conserved role in filopod formation. Proc Natl Acad Sci U S A. 113, E8059–E8068. [PubMed: 27911821]

31. Tokuo H, Mabuchi K, and Ikebe M (2007). The motor activity of myosin-X promotes actin fiber convergence at the cell periphery to initiate filopodia formation. J. Cell Biol. 179, 229–238. [PubMed: 17954606]

32. Masters TA, and Buss F (2017). Filopodia formation and endosome clustering induced by mutant plus-end-directed myosin VI. Proc Natl Acad Sci U S A. 114, 1595–1600. [PubMed: 28143933]

33. He K, Sakai T, Tsukasaki Y, Watanabe TM, and Ikebe M (2017). Myosin X is recruited to nascent focal adhesions at the leading edge and induces multi-cycle filopodial elongation. Sci Rep. 7, 13685. [PubMed: 29057977]

34. Ikebe M, Sato O, and Sakai T (2018). Myosin X and cytoskeletal reorganization. Appl Microsc. 48, 33–42.
35. Arthur AL, Crawford A, Houdusse A, and Titus MA (2021). Vasp mediated actin dynamics recruit and activate filopodia myosin. biorxiv. doi: 10.1101/2021.03.16.435667.
36. Umeki N, Jung HS, Sakai T, Sato O, Ikebe R, and Ikebe M (2011). Phospholipid-dependent regulation of the motor activity of myosin X. Nat. Struct. Biol. 18, 783–788.
37. Plantard L, Arjonen A, Lock JG, Nurani G, Ivaska J, and Stromblad S (2010). PtdIns(3,4,5)P is a regulator of myosin-X localization and filopodia formation. J. Cell Sci. 123, 3525–3534. [PubMed: 20930142]
38. Tokuo H, and Ikebe M (2004). Myosin X transports Mena/VASP to the tip of filopodia. Biochem. Biophys. Res. Commun. 319, 214–220. [PubMed: 15158464]
39. Lin WH, Hurley JT, Raines AN, Cheney RE, and Webb DJ (2013). Myosin X and its motorless isoform differentially modulate dendritic spine development by regulating trafficking and retention of vasodilator-stimulated phosphoprotein. J. Cell Sci. 126, 4756–4768. [PubMed: 23943878]
40. Nagy S, Ricca BL, Norstrom MF, Courson DS, Brawley CM, Smithback PA, and Rock RS (2008). A myosin motor that selects bundled actin for motility. PNAS. 105, 9616–9620. [PubMed: 18599451]
41. Kerber ML, Jacobs DT, Campagnola L, Dunn BD, Yin T, Sousa AD, Quintero OA, and Cheney RE (2009). A novel form of motility in filopodia revealed by imaging Myosin-X at the single-molecule level. Curr. Biol. 19, 967–973. [PubMed: 19398338]
42. Brawley CM, and Rock RS (2009). Unconventional myosin traffic in cells reveals a selective actin cytoskeleton. Proceedings of the National Academy of Science. 106, 9685–9690.
43. Alieva NO, Efremov AK, Hu S, Oh D, Chen Z, Natarajan M, Ong HT, Jégou A, Romet-Lemonne G, Groves JT et al. (2019). Myosin IIA and formin dependent mechanosensitivity of filopodia adhesion. Nat Commun. 10, 3593. [PubMed: 31399564]
44. Almagro S, Durmort C, Chervin-Petinot A, Heyraud S, Dubois M, Lambert O, Maillefaud C, Hewat E, Schaal JP, Huber P et al. (2010). The motor protein Myosin-X transports VE-cadherin along filopodia to allow the formation of early endothelial cell-cell contacts. Mol. Cell. Biol. 30, 1703–1717. [PubMed: 20123970]
45. Zhang H, Berg JS, Li Z, Wang Y, Lang P, Sousa AD, Bhaskar A, Cheney RE, and Stromblad S (2004). Myosin-X provides a motor-based link between integrins and the cytoskeleton. Nat. Cell Biol. 6, 523–531. [PubMed: 15156152]
46. Miihkinen M, Grönloh MLB, Vihinen H, Jokitalo E, Goult BT, Ivaska J, and Jacquemet G (2020). Myosin-X FERM domain modulates integrin activity at filopodia tips. BioRxiv. doi 10.1101/2020.05.05.078733;
47. Efremov AK, Yao M, Sheetz MP, Bershadsky AD, Martinac B, and Yan J (2020). Mechanosensitive calcium signaling in filopodia. bioRxiv. DOI: 10.1038/s41467-019.
48. Bachg AC, Horsthemke M, Skryabin BV, Klasen T, Nagelmann N, Faber C, Woodham E, Machesky LM, Bachg S, Stange R et al. (2019). Phenotypic analysis of Myo10 knockout ($Myo10^{tm2/tm2}$) mice lacking full-length (motorized) but not brain-specific headless myosin X. Sci Rep. 9, 597. [PubMed: 30679680]
49. Heimsath EG, Yim YI, Mustapha M, Hammer JA, and Cheney RE (2017). Myosin-X knockout is semi-lethal and demonstrates that myosin-X functions in neural tube closure, pigmentation, hyaloid vasculature regression, and filopodia formation. Sci Rep. 7, 17354. [PubMed: 29229982]
50. Arjonen A, Kaukonen R, Mattila E, Rouhi P, Högnäs G, Sihto H, Miller BW, Morton JP, Bucher E, Taimen P et al. (2014). Mutant p53-associated myosin-X upregulation promotes breast cancer invasion and metastasis. J. Clin. Invest. 124, 1069–1082. [PubMed: 24487586]
51. Cao R, Chen J, Zhang X, Zhai Y, Qing X, Xing W, Zhang L, Malik YS, Yu H, Zhu X et al. (2014). Elevated expression of myosin X in tumours contributes to breast cancer aggressiveness and metastasis. Br. J. Cancer. 111, 539–550. [PubMed: 24921915]
52. Shibue T, Brooks MW, Inan MF, Reinhardt F, and Weinberg RA (2012). The outgrowth of micrometastases is enabled by the formation of filopodium-like protrusions. Cancer Discov. 2, 706–721. [PubMed: 22609699]

53. Summerbell ER, Mouw JK, Bell JSK, Knippler CM, Pedro B, Arnst JL, Khatib TO, Commander R, Barwick BG, Konen J et al. (2020). Epigenetically heterogeneous tumor cells direct collective invasion through filopodia-driven fibronectin micropatterning. Sci Adv. 6, eaaz6197. [PubMed: 32832657]
54. Tokuo H, Bhawan J, and Coluccio LM (2018). Myosin X is required for efficient melanoblast migration and melanoma initiation and metastasis. Sci Rep. 8, 10449. [PubMed: 29993000]
55. Cordero Cervantes D, and Zurzolo C (2021). Peering into tunneling nanotubes-The path forward. EMBO J. e105789. [PubMed: 33646572]
56. Kornberg TB (2014). Cytonemes and the dispersion of morphogens. Wiley Interdiscip Rev Dev Biol. 3, 445–463. [PubMed: 25186102]
57. Uhl J, Gujarathi S, Waheed AA, Gordon A, Freed EO, and Gousset K (2019). Myosin-X is essential to the intercellular spread of HIV-1 Nef through tunneling nanotubes. J. Cell Commun. Signal. 13, 209–224. [PubMed: 30443895]
58. Gousset K, Marzo L, Commere PH, and Zurzolo C (2013). Myo10 is a key regulator of TNT formation in neuronal cells. J. Cell Sci. 126, 4424–4435. [PubMed: 23886947]
59. Hall ET, Dillard ME, Stewart DP, Zhang Y, Wagner B, Levine RM, Pruett-Miller SM, Sykes A, Temirov J, Cheney RE et al. (2021). Cytoneme delivery of Sonic Hedgehog from ligand-producing cells requires Myosin 10 and a Dispatched-BOC/CDON co-receptor complex. Elife. 10, e61432. [PubMed: 33570491]
60. Liu R, Billington N, Yang Y, Bond C, Hong A, Siththanandan V, Takagi Y, and Sellers JR (2021). A binding protein regulates myosin-7a dimerization and actin bundle assembly. Nat Commun. 12, 563. [PubMed: 33495456]
61. Coluccio LM (2008). Myosin I. In Myosins: A Superfamily of Molecular Motors, Coluccio LM, ed. (Dordrecht, The Netherlands: Springer), pp. 95–124.
62. Nambiar R, McConnell RE, and Tyska MJ (2009). Control of cell membrane tension by myosin-I. Proc Natl Acad Sci U S A. 106, 11972–11977. [PubMed: 19574460]
63. McConnell RE, and Tyska MJ (2007). Myosin-1a powers the sliding of apical membrane along microvillar actin bundles. J. Cell Biol. 177, 671–681. [PubMed: 17502425]
64. McConnell RE, Higginbotham JN, Shifrin DA, Tabb DL, Coffey RJ, and Tyska MJ (2009). The enterocyte microvillus is a vesicle-generating organelle. J. Cell Biol. 185, 1285–1298. [PubMed: 19564407]
65. Tyska MJ, Mackey AT, Huang JD, Copeland NG, Jenkins NA, and Mooseker MS (2005). Myosin-1a is critical for normal brush border structure and composition. Mol. Biol. Cell. 16, 2443–2457. [PubMed: 15758024]
66. Mazzolini R, Dopeso H, Mateo-Lozano S, Chang W, Rodrigues P, Bazzocco S, Alazzouzi H, Landolfi S, Hernandez-Losa J, Andretta E et al. (2012). Brush border Myosin Ia has tumor suppressor activity in the intestine. PNAS. 109, 1530–1535. [PubMed: 22307608]
67. Titus MA (2018). Myosin-driven intracellular transport. Cold Spring Harb Perspect Biol. 10, a021972. [PubMed: 29496823]
68. Hegan PS, Giral H, Levi M, and Mooseker MS (2012). Myosin VI is required for maintenance of brush border structure, composition, and membrane trafficking functions in the intestinal epithelial cell. Cytoskeleton (Hoboken). 69, 235–251. [PubMed: 22328452]
69. Hegan PS, Kravtsov DV, Caputo C, Egan ME, Ameen NA, and Mooseker MS (2015). Restoration of cytoskeletal and membrane tethering defects but not defects in membrane trafficking in the intestinal brush border of mice lacking both myosin Ia and myosin VI. Cytoskeleton (Hoboken). 72, 455–476. [PubMed: 26286357]
70. Crawley SW, Shifrin DA, Grega-Larson NE, McConnell RE, Benesh AE, Mao S, Zheng Y, Zheng QY, Nam KT, Millis BA et al. (2014). Intestinal brush border assembly driven by protocadherin-based intermicrovillar adhesion. Cell. 157, 433–446. [PubMed: 24725409]
71. Weck ML, Crawley SW, Stone CR, and Tyska MJ (2016). Myosin-7b promotes distal tip localization of the intermicrovillar adhesion complex. Curr. Biol. 26, 2717–2728. [PubMed: 27666969]
72. Choi MS, Graves MJ, Matoo S, Storad ZA, El Sheikh Idris RA, Weck ML, Smith ZB, Tyska MJ, and Crawley SW (2020). The small EF-hand protein CALML4 functions as a critical myosin light

chain within the intermicrovillar adhesion complex. J. Biol. Chem. 295, 9281–9296. [PubMed: 32209652]

73. Crawley SW, Weck ML, Grega-Larson NE, Shifrin DA, and Tyska MJ (2016). ANKS4B Is essential for intermicrovillar adhesion complex formation. Dev. Cell. 36, 190–200. [PubMed: 26812018]
74. Li J, He Y, Lu Q, and Zhang M (2016). Mechanistic basis of organization of the harmonin/USH1C-mediated brush border microvilli tip-link complex. Dev. Cell. 36, 179–189. [PubMed: 26812017]
75. Li J, He Y, Weck ML, Lu Q, Tyska MJ, and Zhang M (2017). Structure of Myo7b/USH1C complex suggests a general PDZ domain binding mode by MyTH4-FERM myosins. PNAS. 114, E3776–E3785. [PubMed: 28439001]
76. Yu IM, Planelles-Herrero VJ, Sourigues Y, Moussaoui D, Sirkia H, Kikuti C, Stroebel D, Titus MA, and Houdusse A (2017). Myosin 7 and its adaptors link cadherins to actin. Nat Commun. 8, 15864. [PubMed: 28660889]
77. He Y, Li J, and Zhang M (2019). Myosin VII, USH1C, and ANKS4B or USH1G together form condensed molecular assembly via liquid-liquid phase separation. Cell Rep. 29, 974–986.e4. [PubMed: 31644917]
78. Weck ML, Crawley SW, and Tyska MJ (2020). A heterologous in-cell assay for investigating intermicrovillar adhesion complex interactions reveals a novel protrusion length-matching mechanism. J. Biol. Chem. 295, 16191–16206. [PubMed: 33051206]
79. Henn A, and De La Cruz EM (2005). Vertebrate myosin VIIb is a high duty ratio motor adapted for generating and maintaining tension. J. Biol. Chem. 280, 39665–39676. [PubMed: 16186105]
80. Chinowsky CR, Pinette JA, Meenderink LM, Lau KS, and Tyska MJ (2020). Nonmuscle myosin-2 contractility-dependent actin turnover limits the length of epithelial microvilli. Mol. Biol. Cell. 31, 2803–2815. [PubMed: 33026933]
81. Ebrahim S, Fujita T, Millis BA, Kozin E, Ma X, Kawamoto S, Baird MA, Davidson M, Yonemura S, Hisa Y et al. (2013). NMII forms a contractile transcellular sarcomeric network to regulate apical cell junctions and tissue geometry. Curr. Biol. 23, 731–736. [PubMed: 23562268]
82. Pinette JA, Mao S, Millis BA, Krystofiak ES, Faust JJ, and Tyska MJ (2019). Brush border protocadherin CDHR2 promotes the elongation and maximized packing of microvilli in vivo. Mol. Biol. Cell. 30, 108–118. [PubMed: 30403560]
83. Rzadzinska AK, Schneider ME, Davies C, Riordan GP, and Kachar B (2004). An actin molecular treadmill and myosins maintain stereocilia functional architecture and self-renewal. J. Cell Biol. 164, 887–897. [PubMed: 15024034]
84. McGrath J, Roy P, and Perrin BJ (2017). Stereocilia morphogenesis and maintenance through regulation of actin stability. Semin. Cell. Dev. Biol. 65, 88–95. [PubMed: 27565685]
85. Richardson GP, and Petit C (2019). Hair-bundle links: genetics as the gateway to function. Cold Spring Harb Perspect Med. 9, a033142. [PubMed: 30617060]
86. Tarchini B, and Lu X (2019). New insights into regulation and function of planar polarity in the inner ear. Neurosci. Lett. 709, 134373. [PubMed: 31295539]
87. Krey JF, Chatterjee P, Dumont RA, O'Sullivan M, Choi D, Bird JE, and Barr-Gillespie PG (2020). Mechanotransduction-dependent control of stereocilia dimensions and row identity in inner hair cells. Curr. Biol. 30, 442–454.e7. [PubMed: 31902726]
88. Velez-Ortega AC, and Frolenkov GI (2019). Building and repairing the stereocilia cytoskeleton in mammalian auditory hair cells. Hear Res. 376, 47–57. [PubMed: 30638948]
89. Elliott KL, Fritzsch B, and Duncan JS (2018). Evolutionary and developmental biology provide insights into the regeneration of Organ of Corti hair cells. Front Cell Neurosci. 12, 252. [PubMed: 30135646]
90. Maoileidigh DO, and Ricci AJ (2019). A bundle of mechanisms: inner-ear hair-cell mechanotransduction. Trends Neurosci. 42, 221–236. [PubMed: 30661717]
91. Gillespie PG, and Muller U (2009). Mechanotransduction by hair cells: models, molecules, and mechanisms. Cell. 139, 33–44. [PubMed: 19804752]
92. Shin JB, Krey JF, Hassan A, Metlagel Z, Tauscher AN, Pagana JM, Sherman NE, Jeffery ED, Spinelli KJ, Zhao H et al. (2013). Molecular architecture of the chick vestibular hair bundle. Nat. Neurosci. 16, 365–374. [PubMed: 23334578]

93. Grati M, and Kachar B (2011). Myosin VIIa and sans localization at stereocilia upper tip-link density implicates these Usher syndrome proteins in mechanotransduction. PNAS. 108, 11476–11481. [PubMed: 21709241]

94. Kros CJ, Marcotti W, van Netten SM, Self TJ, Libby RT, Brown SDM, Richardson GP, and Steel KP (2002). Reduced climbing and increased slipping adaptation in cochlear hair cells of mice with Myo7a mutations. Nat. Neurosci. 5, 41–47. [PubMed: 11753415]

95. Li S, Mecca A, Kim J, Caprara GA, Wagner EL, Du TT, Petrov L, Xu W, Cui R, Rebustini IT et al. (2020). Myosin-VIIa is expressed in multiple isoforms and essential for tensioning the hair cell mechanotransduction complex. Nat Commun. 11, 2066. [PubMed: 32350269]

96. Laakso JM, Lewis JH, Shuman H, and Ostap EM (2010). Control of myosin-I force sensing by alternative splicing. PNAS. 107, 698–702. [PubMed: 20080738]

97. Robert-Paganin J, Robblee JP, Auguin D, Blake TCA, Bookwalter CS, Krementsova EB, Moussaoui D, Previs MJ, Jousset G, Baum J et al. (2019). *Plasmodium* myosin A drives parasite invasion by an atypical force generating mechanism. Nature Comm. 10, 3286.

98. Goodyear R, and Richardson G (1999). The ankle-link antigen: an epitope sensitive to calcium chelation associated with the hair-cell surface and the calycal processes of photoreceptors. J. Neurosci. 19, 3761–3772. [PubMed: 10234008]

99. Boëda B, El-Amraoui A, Bahloul A, Goodyear R, Daviet L, Blanchard S, Perfettini I, Fath KR, Shorte S, Reiners J et al. (2002). Myosin VIIa, harmonin and cadherin 23, three Usher 1 gene products that cooperate to shape the sensory hair bundle. EMBO Journal. 21, 6689–6699.

100. Morgan CP, Krey JF, Grati M, Zhao B, Fallen S, Kannan-Sundhari A, Liu XZ, Choi D, Müller U, and Barr-Gillespie PG (2016). PDZD7-MYO7A complex identified in enriched stereocilia membranes. Elife. 5, e18312. [PubMed: 27525485]

101. Gibson F, Walsh J, Mburu P, Varela A, Brown KA, Antonio M, Beisel KW, Steel KP, and Brown SDM (1995). A type VII myosin encoded by the mouse deafness gene *shaker-1*. Nature. 374, 62–64. [PubMed: 7870172]

102. Weil D, Blanchard S, Kaplan J, Guliford P, Gibson F, Walsh J, Mburu P, Varela A, Levilliers J, Weston MD et al. (1995). Defective myosin VIIA gene responsible for Usher syndrome type 1B. Nature. 374, 60–61. [PubMed: 7870171]

103. Nicolson T, Rüsch A, Friedrich RW, Granato M, Ruppersberg JP, and Nüsslein-Volhard C (1999). Genetic analysis of vertebrate sensory hair cell mechanosensation: the zebrafish circler mutants. Neuron. 20, 271–283.

104. Self T, Mahony M, Fleming J, Walsh J, Brown SDM, and Steel KP (1998). Shaker-1 mutations reveal roles for myosin VIIA in both development and function of cochlear hair cells. Development. 125, 557–566. [PubMed: 9435277]

105. Pan L, Yan J, Wu L, and Zhang M (2009). Assembling stable hair cell tip link complex via multidentate interactions between harmonin and cadherin 23. PNAS. 106, 5575–5580. [PubMed: 19297620]

106. Wu L, Pan L, Wei Z, and Zhang M (2011). Structure of MyTH4-FERM domains in myosin VIIa tail bound to cargo. Science. 331, 757–760. [PubMed: 21311020]

107. Bahloul A, Pepermans E, Raynal B, Wolff N, Cordier F, England P, Nouaille S, Baron B, El-Amraoui A, Hardelin JP et al. (2017). Conformational switch of harmonin, a submembrane scaffold protein of the hair cell mechanoelectrical transduction machinery. FEBS Lett. 591, 2299–2310. [PubMed: 28653419]

108. Grillet N, Xiong W, Reynolds A, Kazmierczak P, Sato T, Lillo C, Dumont RA, Hintermann E, Sczaniecka A, Schwander M et al. (2009). Harmonin mutations cause mechanotransduction defects in cochlear hair cells. Neuron. 62, 375–387. [PubMed: 19447093]

109. Michalski N, Michel V, Caberlotto E, Lefèvre GM, van Aken AF, Tinevez JY, Bizard E, Houbron C, Weil D, Hardelin JP et al. (2009). Harmonin-b, an actin-binding scaffold protein, is involved in the adaptation of mechanoelectrical transduction by sensory hair cells. Pflugers Arch. 459, 115–130. [PubMed: 19756723]

110. Verpy E, Leibovici M, Zwaenepoel I, Liu XZ, Gal A, Salem N, Mansour A, Blanchard S, Kobayashi I, Keats BJ et al. (2000). A defect in harmonin, a PDZ domain-containing protein

expressed in the inner ear sensory hair cells, underlies Usher syndrome type 1C. Nat. Genet. 26, 51–55. [PubMed: 10973247]

111. Yan J, Pan L, Chen X, Wu L, and Zhang M (2010). The structure of the harmonin/sans complex reveals an unexpected interaction mode of the two Usher syndrome proteins. PNAS. 107, 4040–4045. [PubMed: 20142502]
112. Krey JF, and Barr-Gillespie PG (2019). Molecular Composition of Vestibular Hair Bundles. Cold Spring Harb Perspect Med. 9, a033209. [PubMed: 29844221]
113. Zhu Y, Scheibinger M, Ellwanger DC, Krey JF, Choi D, Kelly RT, Heller S, and Barr-Gillespie PG (2019). Single-cell proteomics reveals changes in expression during hair-cell development. Elife. 8, e50777. [PubMed: 31682227]
114. Sakai T, Jung HS, Sato O, Yamada MD, You DJ, Ikebe R, and Ikebe M (2015). Structure and Regulation of the Movement of Human Myosin VIIA. J. Biol. Chem. 290, 17587–17598. [PubMed: 26001786]
115. Sakai T, Umeki N, Ikebe R, and Ikebe M (2011). Cargo binding activates myosin VIIA motor function in cells. PNAS. 108, 7028–7033. [PubMed: 21482763]
116. Michalski N, Michel V, Bahloul A, Lefèvre G, Barral J, Yagi H, Chardenoux S, Weil D, Martin P, Hardelin JP et al. (2007). Molecular characterization of the ankle-link complex in cochlear hair cells and its role in the hair bundle functioning. J. Neurosci. 27, 6478–6488. [PubMed: 17567809]
117. Zou J, Chen Q, Almishaal A, Mathur PD, Zheng T, Tian C, Zheng QY, and Yang J (2017). The roles of USH1 proteins and PDZ domain-containing USH proteins in USH2 complex integrity in cochlear hair cells. Hum. Mol. Genet. 26, 624–636. [PubMed: 28031293]
118. Zou J, Mathur PD, Zheng T, Wang Y, Almishaal A, Park AH, and Yang J (2015). Individual USH2 proteins make distinct contributions to the ankle link complex during development of the mouse cochlear stereociliary bundle. Hum. Mol. Genet. 24, 6944–6957. [PubMed: 26401052]
119. Ebermann I, Phillips JB, Liebau MC, Koenekoop RK, Schermer B, Lopez I, Schäfer E, Roux AF, Dafinger C, Bernd A et al. (2010). PDZD7 is a modifier of retinal disease and a contributor to digenic Usher syndrome. J. Clin. Invest. 120, 1812–1823. [PubMed: 20440071]
120. Mburu P, Mustapha M, Varela A, Weil D, El-Amraoui A, Holme RH, Rump A, Hardisty RE, Blanchard S, Coimbra RS et al. (2003). Defects in whirlin, a PDZ domain molecule involved in stereocilia elongation, cause deafness in the whirler mouse and families with DFNB31. Nat. Genet. 34, 421–428. [PubMed: 12833159]
121. Küssel-Andermann P, El-Amraoui A, Safieddine S, Nouaille S, Perfettini I, Lecuit M, Cossart P, Wolfrum U, and Petit C (2000). Vezatin, a novel transmembrane protein, bridges myosin VIIA to the cadherin-catenins complex. EMBO J. 19, 6020–6029. [PubMed: 11080149]
122. Avraham KB, Hasson T, Steel KP, Kingsley DM, Russell LB, Mooseker MS, Copeland NG, and Jenkins NA (1995). The mouse *Snell's waltzer* deafness gene encodes an unconventional myosin required for structural integrity of inner ear hair cells. Nat. Genet. 11, 369–375. [PubMed: 7493015]
123. Hasson T, Gillespie PG, Garcia JA, MacDonald RB, Zhao Y, Yee AG, Mooseker MS, and Corey DP (1997). Unconventional myosins in inner-ear sensory epithelia. J. Cell Biol. 137, 1287–1307. [PubMed: 9182663]
124. Self T, Sobe T, Copeland NG, Jenkins NA, Avraham KB, and Steel KP (1999). Role of myosin VI in the differentiation of cochlear hair cells. Dev. Biol. 214, 331–341. [PubMed: 10525338]
125. Sakaguchi H, Tokita J, Naoz M, Bowen-Pope D, Gov NS, and Kachar B (2008). Dynamic compartmentalization of protein tyrosine phosphatase receptor Q at the proximal end of stereocilia: implication of myosin VI-based transport. Cell Motil. Cytoskeleton. 65, 528–538. [PubMed: 18412156]
126. Salles FT, Andrade LR, Tanda S, Grati M, Plona KL, Gagnon LH, Johnson KR, Kachar B, and Berryman MA (2014). CLIC5 stabilizes membrane-actin filament linkages at the base of hair cell stereocilia in a molecular complex with radixin, taperin, and myosin VI. Cytoskeleton (Hoboken). 71, 61–78. [PubMed: 24285636]
127. Seki Y, Miyasaka Y, Suzuki S, Wada K, Yasuda SP, Matsuoka K, Ohshiba Y, Endo K, Ishii R, Shitara H et al. (2017). A novel splice site mutation of myosin VI in mice leads to stereociliary

fusion caused by disruption of actin networks in the apical region of inner ear hair cells. PLoS One. 12, e0183477. [PubMed: 28832620]

128. Cirilo JA, Gunther LK, and Yengo CM (2021). Functional role of class III myosins in hair cells. Front Cell Dev Biol. 9, 643856. [PubMed: 33718386]
129. Quintero OA, Unrath WC, Stevens SMJ, Manor U, Kachar B, and Yengo CM (2013). Myosin 3A kinase activity is regulated by phosphorylation of the kinase domain activation loop. J. Biol. Chem. 288, 37126–37137. [PubMed: 24214986]
130. Raval MH, Quintero OA, Weck ML, Unrath WC, Gallagher JW, Cui R, Kachar B, Tyska MJ, and Yengo CM (2016). Impact of the motor and tail domains of class III myosins on regulating the formation and elongation of actin protrusions. J. Biol. Chem. 291, 22781–22792. [PubMed: 27582493]
131. Salles FT, Merritt RCJ, Manor U, Dougherty GW, Sousa AD, Moore JE, Yengo CM, Dose AC, and Kachar B (2009). Myosin IIIa boosts elongation of stereocilia by transporting espin 1 to the plus ends of actin filaments. Nat. Cell Biol. 11, 443–350. [PubMed: 19287378]
132. Erickson FL, Corsa AC, Dosé A, and Burnside B (2003). Localization of a class III myosin to filopodia tips in transfected HeLa cells. Mol. Biol. Cell. 14, 4173–4180. [PubMed: 14517327]
133. Merritt RC, Manor U, Salles FT, Grati M, Dosé AC, Unrath WC, Quintero OA, Yengo CM, and Kachar B (2012). Myosin IIIB uses an actin-binding motif in Its espin-1 cargo to reach the tips of actin protrusions. Curr. Biol. 22, 320–325. [PubMed: 22264607]
134. Liu H, Li J, Raval MH, Yao N, Deng X, Lu Q, Nie S, Feng W, Wan J, Yengo CM et al. (2016). Myosin III-mediated cross-linking and stimulation of actin bundling activity of Espin. Elife. 5, e12856. [PubMed: 26785147]
135. Ebrahim S, Avenarius MR, Grati M, Krey JF, Windsor AM, Sousa AD, Ballesteros A, Cui R, Millis BA, Salles FT et al. (2016). Stereocilia-staircase spacing is influenced by myosin III motors and their cargos espin-1 and espin-like. Nat Commun. 7, 10833. [PubMed: 26926603]
136. Schneider ME, Dose AC, Salles FT, Chang W, Erickson FL, Burnside B, and Kachar B (2006). A new compartment at stereocilia tips defined by spatial and temporal patterns of myosin IIIa expression. J. Neurosci. 26, 10243–10252. [PubMed: 17021180]
137. Lelli A, Michel V, Boutet de Monvel J, Cortese M, Bosch-Grau M, Aghaie A, Perfettini I, Dupont T, Avan P, El-Amraoui A et al. (2016). Class III myosins shape the auditory hair bundles by limiting microvilli and stereocilia growth. J. Cell Biol. 212, 231–244. [PubMed: 26754646]
138. Walsh T, Walsh V, Vreugde S, Hertzano R, Shahin H, Haika H, Lee MK, Kanaan M, King MC, and Avraham KB (2002). From flie's eyes to our ears: mutations in a human class III myosin cause progressive nonsyndromic hearing loss DFNB30. PNAS. 99, 7518–7523. [PubMed: 12032315]
139. Walsh VL, Raviv D, Dror AA, Shahin H, Walsh T, Kanaan MN, Avraham KB, and King MC (2010). A mouse model for human hearing loss DFNB30 due to loss of function of myosin IIIA. Mamm Genome. 22, 170–177. [PubMed: 21165622]
140. Belyantseva IA, Boger ET, and Friedman TB (2003). Myosin XVa localizes to the tips of inner ear sensory cell stereocilia and is essential for staircase formation of the hair bundle. PNAS. 100, 13958–13963. [PubMed: 14610277]
141. Probst FJ, Fridell RA, Raphael Y, Saunders TL, Wang A, Liang Y, Morell RJ, Touchman JW, Lyons RH, Noben-Trauth K et al. (1998). Correction of deafness in *shaker-2* mice by an unconventional myosin in a BAC transgene. Science. 280, 1444–1447. [PubMed: 9603735]
142. Bird JE, Barzik M, Drummond MC, Sutton DC, Goodman SM, Morozko EL, Cole SM, Boukhvalova AK, Skidmore J, Syam D et al. (2017). Harnessing molecular motors for nanoscale pulldown in live cells. Mol. Biol. Cell. 28, 463–475. [PubMed: 27932498]
143. Jiang F, Takagi Y, Shams A, Heissler SM, Friedman TB, Sellers JR, and Bird JE (2021). The ATPase mechanism of myosin 15, the molecular motor mutated in DFNB3 human deafness. J. Biol. Chem. 296, 100243. [PubMed: 33372036]
144. Belyantseva IA, Boger ET, Naz S, Frolenkov GI, Sellers JR, Ahmed ZM, Griffith AJ, and Friedman TB (2005). Myosin-XVa is required for tip localization of whirlin and differential elongation of hair-cell stereocilia. Nat. Cell Biol. 7, 148–156. [PubMed: 15654330]

145. Liang Y, Wang A, Belyantseva IA, Anderson DW, Probst FJ, Barber TD, Miller W, Touchman JW, Jin L, Sullivan SL et al. (1999). Characterization of the human and mouse unconventional myosin XV genes responsible for hereditary deafness DFNB3 and *shaker 2*. Genomics. 61, 243–258. [PubMed: 10552926]

146. Fang Q, Indzhykulian AA, Mustapha M, Riordan GP, Dolan DF, Friedman TB, Belyantseva IA, Frolenkov GI, Camper SA, and Bird JE (2015). The 133-kDa N-terminal domain enables myosin 15 to maintain mechanotransducing stereocilia and is essential for hearing. Elife. 4, e08627.

147. Delprat B, Michel V, Goodyear R, Yamasaki Y, Michalski N, El-Amraoui A, Perfettini I, Legrain P, Richardson G, Hardelin JP et al. (2005). Myosin XVa and whirlin, two deafness gene products required for hair bundle growth, are located at the stereocilia tips and interact directly. Hum. Mol. Genet. 14, 401–410. [PubMed: 15590698]

148. Manor U, Disanza A, Grati M, Andrade L, Lin H, Di Fiore PP, Scita G, and Kachar B (2011). Regulation of stereocilia length by myosin XVa and whirlin depends on the actin-regulatory protein Eps8. Curr. Biol. 21, 167–172. [PubMed: 21236676]

149. Mauriac SA, Hien YE, Bird JE, Carvalho SD, Peyroutou R, Lee SC, Moreau MM, Blanc JM, Geyser A, Medina C et al. (2017). Defective Gpsm2/Gα^{i3} signalling disrupts stereocilia development and growth cone actin dynamics in Chudley-McCullough syndrome. Nat Commun. 8, 14907. [PubMed: 28387217]

150. Tadenev ALD, Akturk A, Devanney N, Mathur PD, Clark AM, Yang J, and Tarchini B (2019). GPSM2-GNAI specifies the tallest stereocilia and defines hair bundle row identity. Curr. Biol. 29, 921–934.e4. [PubMed: 30827920]

151. Lin L, Shi Y, Wang M, Wang C, Lu Q, Zhu J, and Zhang R (2021). Phase separation-mediated condensation of Whirlin-Myo15-Eps8 stereocilia tip complex. Cell Rep. 34, 108770. [PubMed: 33626355]

152. Frolenkov GI, Belyantseva IA, Friedman TB, and Griffith AJ (2004). Genetic insights into the morphogenesis of inner ear hair cells. Nat. Rev. Genet. 5, 489–498. [PubMed: 15211351]

153. Hadi S, Alexander AJ, Vélez-Ortega AC, and Frolenkov GI (2020). Myosin-XVa controls both staircase architecture and diameter gradation of stereocilia rows in the auditory hair cell bundles. J Assoc Res Otolaryngol. 21, 121–135. [PubMed: 32152769]

154. Biyasheva A, Svitkina T, Kunda P, Baum B, and Borisy G (2004). Cascade pathway of filopodia formation downstream of SCAR. J. Cell Sci. 117, 837–848. [PubMed: 14762109]

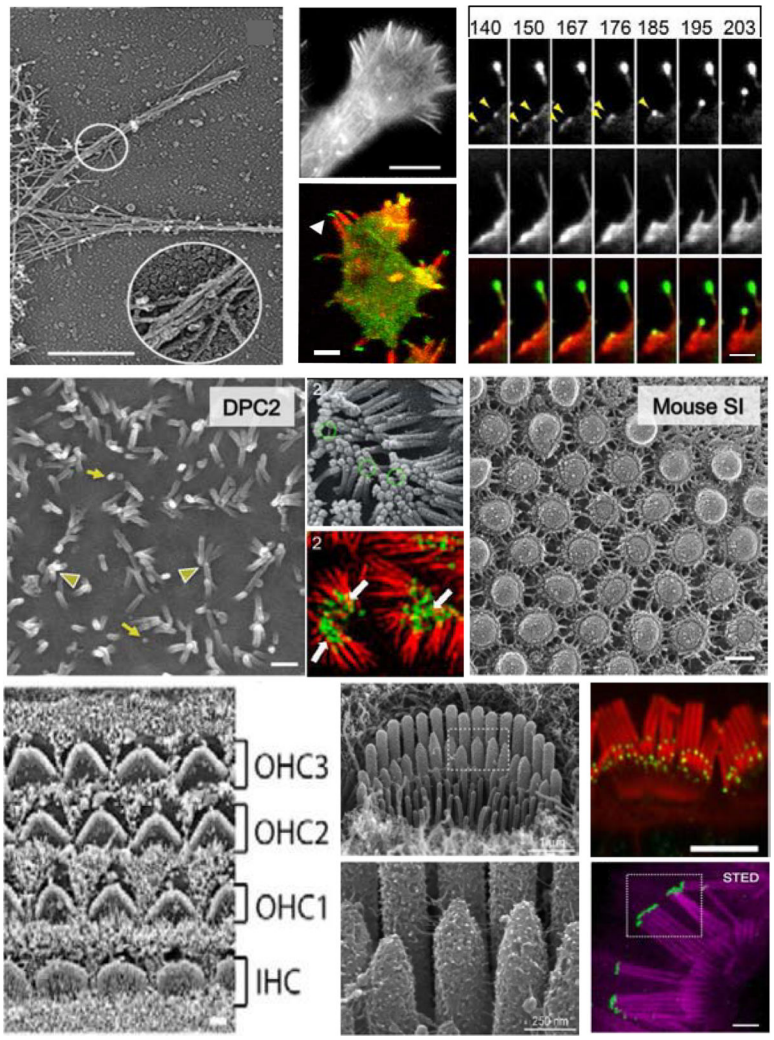

Figure 1. Features of filopodia, microvilli and stereocilia.

(A) Platinum replica micrograph of a filopodium extending from the lamella of a BG2 cell, scale = 1μm. (B) Filopodia emerging from the lamella of a BG2 fly neural cell, scale = 1μm. (C) *Dictyostelium* amoeba expressing GFP-DdMYO7 stained with phalloidin, scale = 5 μm. (D) Time course (in sec) of HeLa cell expressing EGFP-MYO10 (top) and mCherry-actin (middle) extending a filopodium, showing punctae assembling on the membrane that gives rise to a new filopodium, scale = 2 μm. (E) Scanning EM of the apical surface of differentiating Caco2BBE cells 2 days post confluency (DPC) showing microvilli buds (yellow arrows) and longer microvilli clustered at their tips (arrowheads), scale = 500 nm. (F) SEM at 8 DPC showing clustering of microvilli tips and the links between them (green circles), scale = each side is 50 μm. (G) Structured illumination microscopy of CACO-2BBE cells expressing EGFP-MYO7B (green) stained for F-actin (red). Distal tip enrichment is indicated by arrowheads, scale = each side is 50 μm. (H) Freeze-etch EM of apical surface of the mouse small intestine showing the organization of linked microvilli, scale = 100 nm. (I) SEM of the auditory epithelium from a P8 mouse showing the organization of the outer and inner hair cells (OHC, IHC), scale = 1 μm. (J) SEM of IHC stereocilia at P4, boxed region at top is shown below. Note the inter-stereocilia links. (K) IHC stained for MYO15-L (green -

tips of row 2 and 3) and actin (red), scale = 500 nm. (L) STED microscopy showing actin (purple) and GPSM2 (green) localized to the tip of row 1 stereocilia, scale = 2 μm. (A,B) [154] (C) [6] (D) [33] (E, H) [70] (F, G) [71] (I) (J,K)[146] (L) [149].

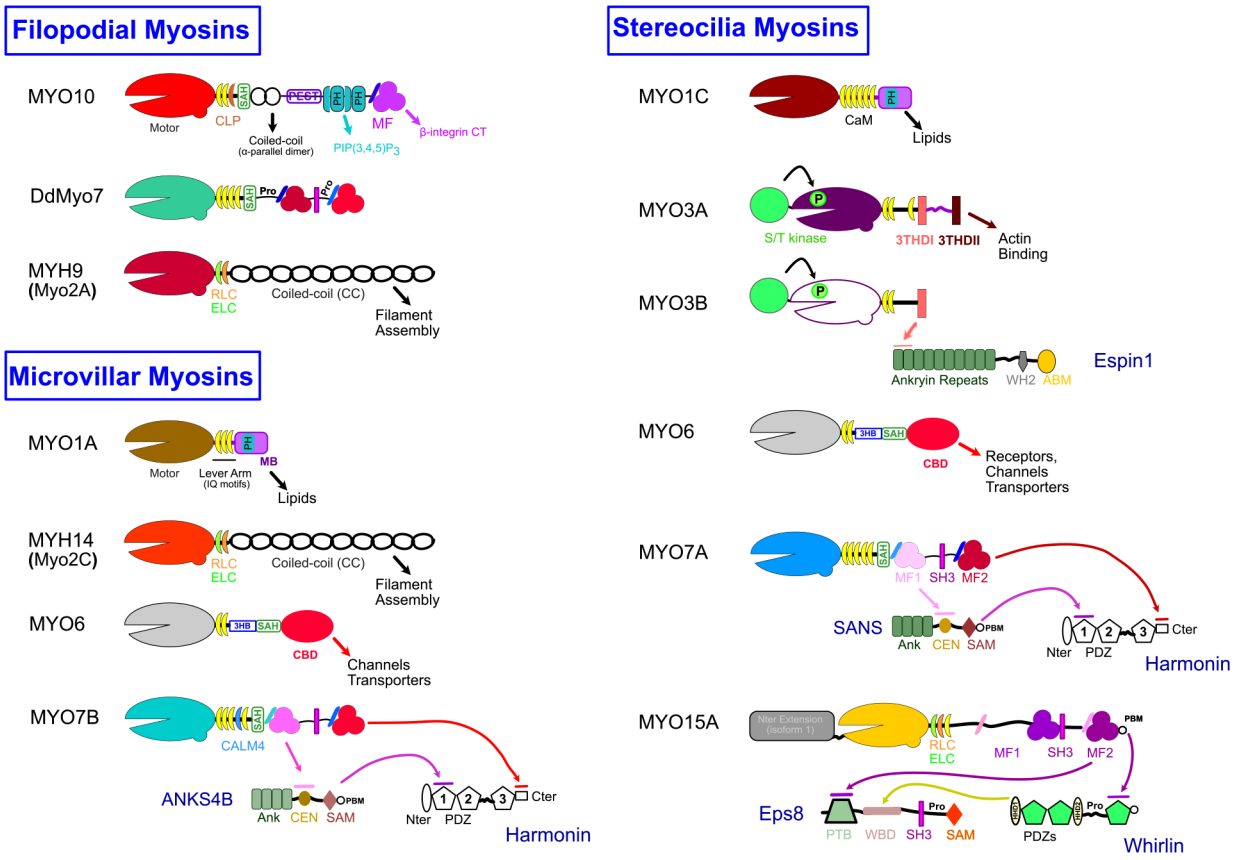

Figure 2. Myosin family members with roles in Filopodia, Microvilli and Stereocilia.

Cartoon schematics illustrating the key domains and features of diverse myosin motors. Key features are annotated and interactions between domains and partners or targets are indicated with arrows. Note that some myosins may use other light chains (LCs) in addition to calmodulin (CaM), including essential and regulatory LCs (**ELC**, **RLC**), calmodulin-related LC (**CALM4**, **CLP**). **SAH**, stable α-helix; **PEST**, proline (P), glutamic acid (E), serine (S), and threonine (T) rich sequence; **PH**, plekstrin homology; **MF**, MyTH4-FERM; $PIP(3,4,5)P_3$, Phosphatidylinositol (3,4,5)-trisphosphate; **MB**, membrane binding; **3HB**, three-helix bundle; **CBD**, cargo binding domain; **S/T kinase**, serine/threonine kinase; **3THDI/II**, tail homology domain I or II; **SH3**, src homology 3; **CT**, cytoplasmic tail; **Ank**, Ankryin repeat region; **CEN**, central domain; **SAM**, sterile alpha motif; **PBM**, PDZ binding motif; **Nter**/**Cter**, N-terminus and C-terminus; **PDZ**, post synaptic density protein (PSD95), Drosophila disc large tumor suppressor (Dlg1), and zonula occludens-1 protein (zo-1); **WH2**, Wasp homology 2; **ABM**, actin binding module; **PTB**, phosphotyrosine binding domain; **WBD**, whirlin binding domain; Pro, Proline-rich; **HHD**, harmonin homology domain.

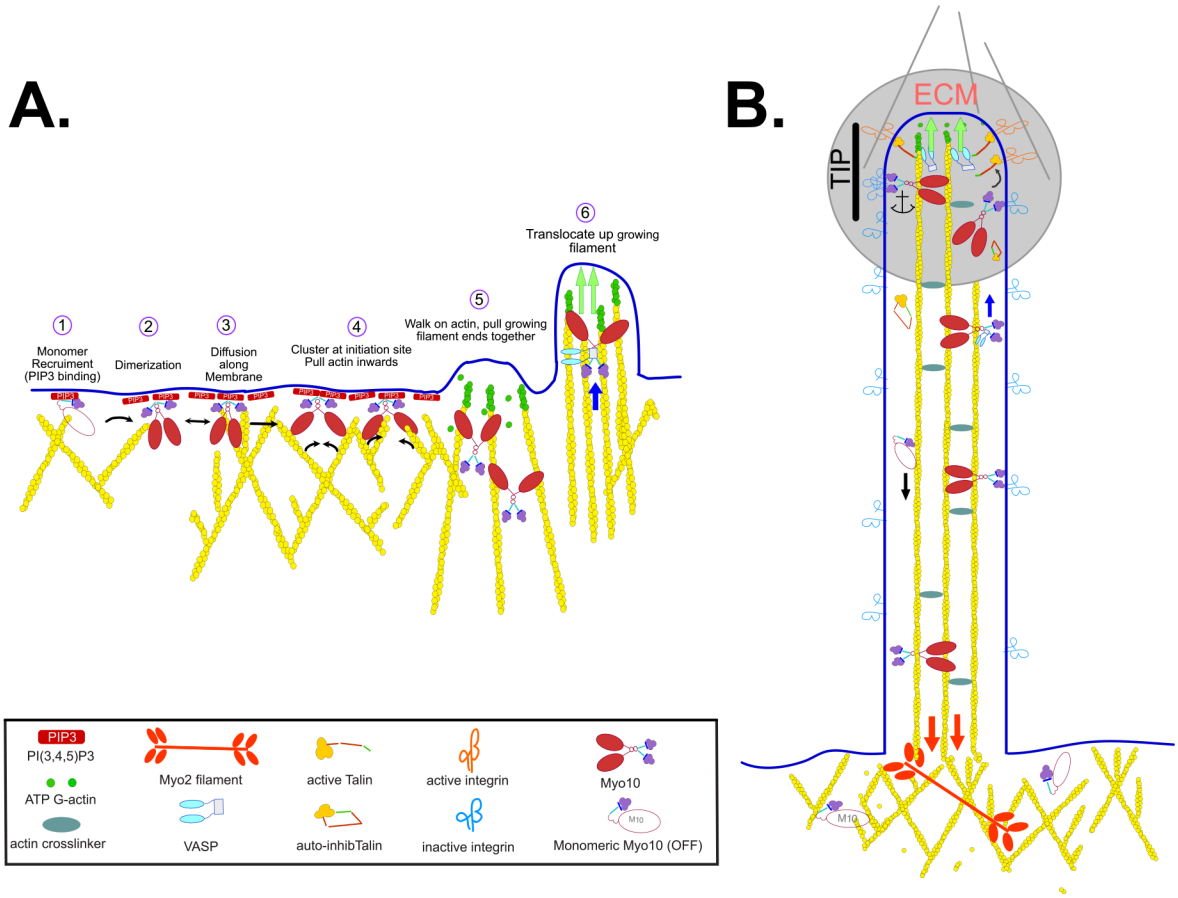

Figure 3. Model of MYO10 Function in Filopodia Formation and Function.

Schematic illustration of the activation and role of MYO10 in filopodia initiation, in transport of VASP towards the growing filopodia tip and in anchoring integrins at the filopodia tip. **(A)** MYO10 is a monomer prior to activation and binding to PI(3,4,5)P3 opens the molecule and promotes activation and dimerization (illustrated on the left side). Green arrows indicate extension of filopodium as monomers are added to the tip of the growing filopodium. Blue arrow represents myosin-driven transport of a cargo. **(B)** MYO10 within the filopodium can translocate along the actin core or return to the cytosol via retrograde flow generated by MYO2A. Red arrows indicate the downward pulling force exerted by MYO2A filaments in the cortex. ECM, extracellular matrix (highlighted with grey circle).

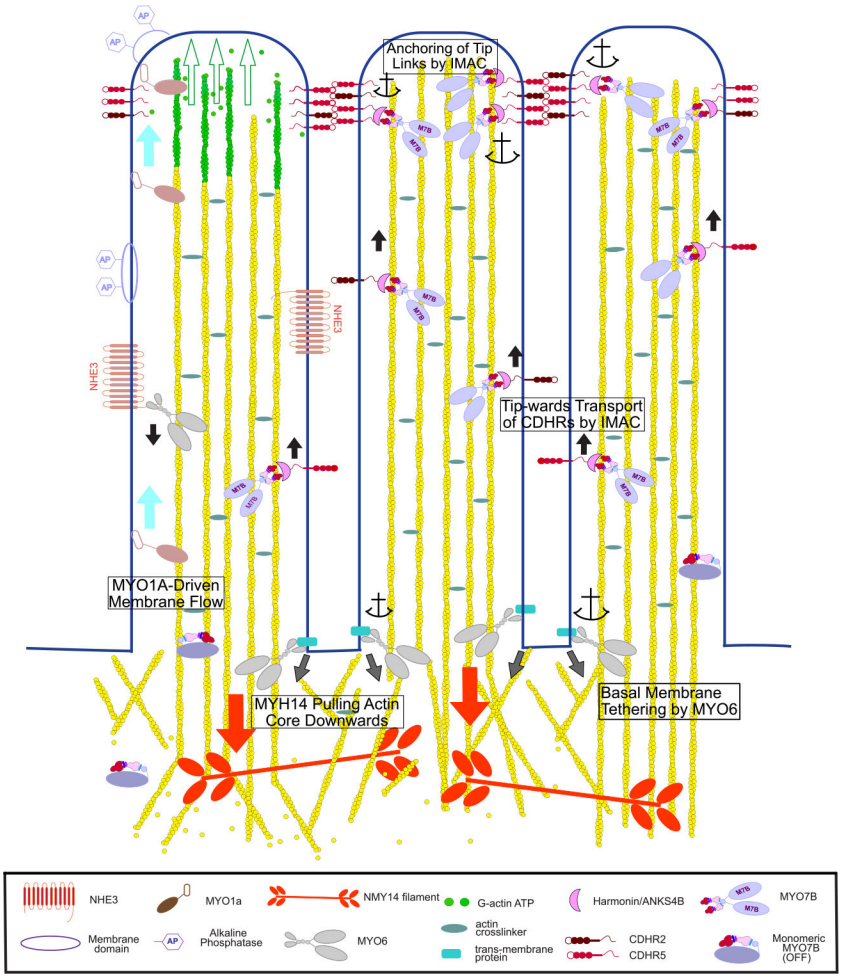

Figure 4. The Myosins of Microvilli.

Conceptual model of the diverse functions carried out by the different microvillar myosins. These include generation of membrane flow by MYO1A (light blue arrows) that leads to shedding of membrane vesicles containing alkaline phosphatase (AP). Green arrows indicate extension of microvillus as monomers are added to the tip. MYO6 transports channels down to the base of the microvillus, such as NHE3 as shown here, and also keeps the basal plasma membrane between the microvilli tightly anchored to the actin cortex (grey arrows). MYO7B-Harmonin-ANKSB may move component of the IMAC complex including Harmonin, ANKS4B, CDHR2 and CDHR5 cadherin up toward the microvilli tip (black arrows). There, an IMAC condensate that includes MYO7B could anchor the cadherins in place thus stabilizing the inter-microvilli links. Non-muscle MYO2C links actin rootlets and provides a downward pulling force (red arrows) balanced by polymerization at the microvilli tip to maintain proper microvilli length.

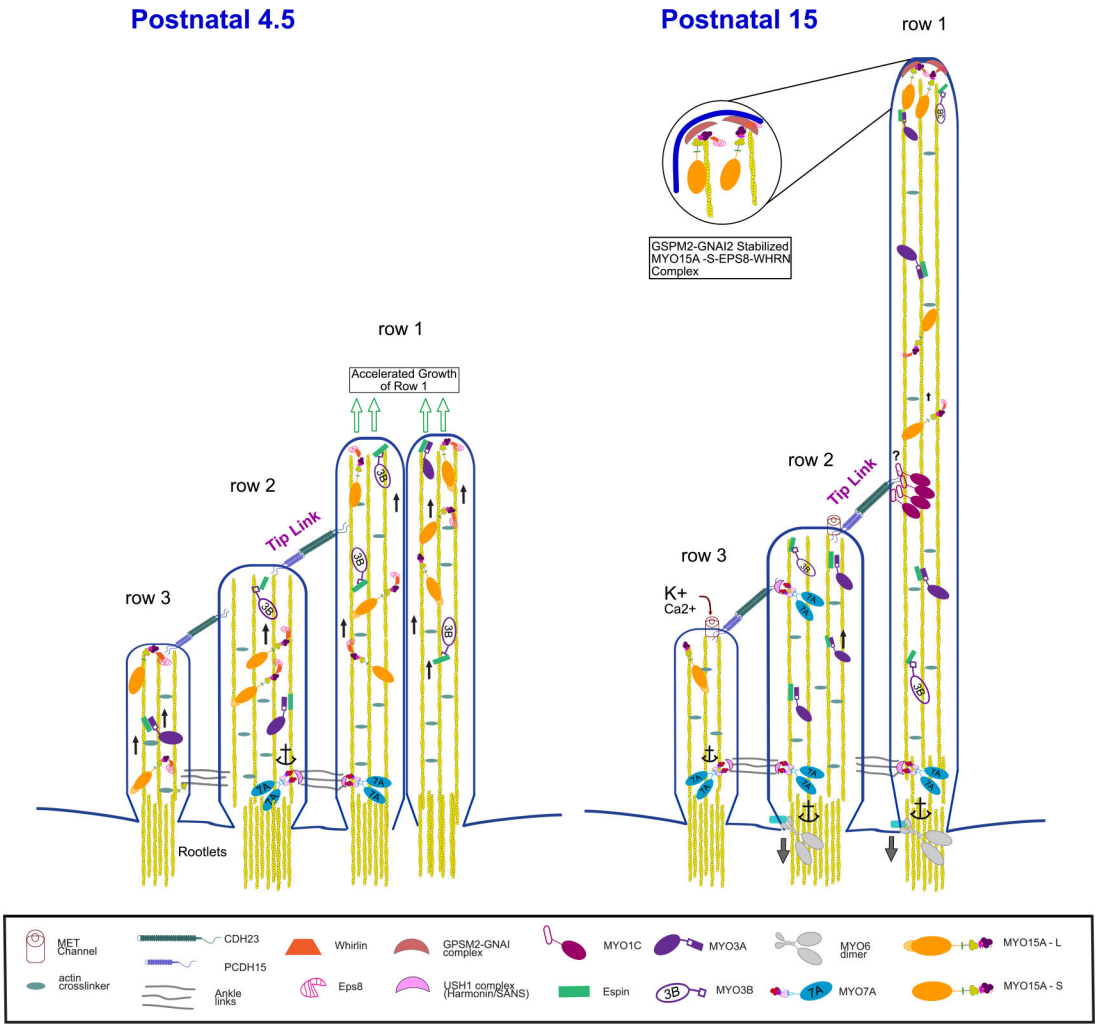

Figure 5. Functions of Stereocilia Myosins.

Diagram illustrating the roles of myosins in controlling the length of stereocilia, linking adjacent stereocilia and anchoring the tip link at postnatal day 4.5 (left) and postnatal day 15 (right). MYO3A/B play a role in the transport of the actin bundling protein ESPN that regulates the length of the growing stereocilia. MYO15A also acts as a transporter, carrying the adaptor WHRN and the actin regulator Eps8 to the tips of all stereocilia at P4.5 to promote stereocilia growth. The long isoform MYO15A-L is localized most notably in row 1 (green arrows) at P15 where it forms with Eps8 and WHRN a complex with GPSM2-GNAI complex that stimulates actin polymerization activity and drives stereocilia elongation. In contrast, the short MYO15A-S isoform is found only in rows 2 and 3 where it stabilizes these shorter stereocilia. Several MYO1C are likely associated at the upper tip link density, clustered by an unknown mechanism (indicated by **?**) where it contributes to slow adaptation. MYO7A is also present at the upper tip link density where it serves as the tip link motor, tensioning the MET channel. MYO7A also associates with ankle links that contribute to holding the hair bundle together. MYO6 is concentrated at the base of the

stereocilia in the actin-dense rootlets where it anchors the membrane to the actin-rich cuticular plate (not shown).